A STUDY OF THERMALLY STIMULATED LUMINESCENCE AND THERMALLY STIMULATED CHARGE EMISSION IN $KMgF_3$

By

JAMES ANTHONY MACINERNEY
II

Bachelor of Science
University College
Dublin, Ireland
1962

Master of Science
Oklahoma State University
Stillwater, Oklahoma
1969

Submitted to the Faculty of the Graduate College
of the Oklahoma State University
in partial fulfillment of the requirements
for the Degree of
DOCTOR OF PHILOSOPHY
July, 1974

A STUDY OF THERMALLY STIMULATED LUMINESCENCE AND THERMALLY STIMULATED CHARGE EMISSION IN $KMgF_3$

Thesis Approved:

Thesis Adviser

Paul Westhaus

William J. Lewis

Tom E. Moore

Dean of the Graduate College

ACKNOWLEDGMENTS

I want to thank my adviser, Dr. Elton E. Kohnke, for his patience, guidance, and constant help throughout the course of this study. My thanks go to Dr. W. A. Sibley for supplying $KMgF_3$ crystals and use of emission spectroscopy equipment. To Mr. Heinz Hall, Mr. Wayne Atkins, and associates goes my appreciation for their skilled technical help and advice. Gratitude is expressed to Dr. Larry E. Halliburton for taking the EPR data which helped significantly in making a model for the TSL. To him also and to Dr. Soo In Yun go my thanks for many helpful conversations. I wish to thank Dr. A. D. Souder of Seneca College for his critical reading of the manuscript and much helpful advice. I acknowledge financial assistance in the form of a research assistantship from the National Science Foundation in the summer of 1972 and a teaching assistantship from the Physics Department of Oklahoma State University. In conclusion I wish to thank Norma for her encouragement and for typing the manuscript.

TABLE OF CONTENTS

Chapter Page

V. (CONTINUED)

LIST OF FIGURES

Figure Page

CHAPTER I

INTRODUCTION

Information on the properties of defects in solids is important in practical work, especially in the semi-conductor industry. In recent years, however, there is some demand for special materials with known electrical, optical, and mechanical properties. Areas requiring these special materials include electro-optical devices, computer memory storage, high temperature applications in space, and radiation damage in the nuclear industry.

Many techniques are available for characterizing these properties of solids. Among these are thermoluminescence (TL), Electron Paramagnetic Resonance (EPR), and Optical Absorption (OA). Thermoluminescence, perhaps more correctly called Thermally Stimulated Luminescence (TSL), has been used as a basis for a radiation dosimeter technique widely applied in measuring exposures in nuclear reactor personnel and in cancer treatment (1).

Thermoluminescence has been known for many years and occurs in a wide variety of organic and inorganic materials. For a long time, the only type of work done was descriptive; and no attempt was made to understand the mechanism involved. In recent years, increasing emphasis has been placed by Dutton and Maurer (2) and Merz and Pershan (3) on combining EPR and optical absorption to probe radiation damage, electron trapping, and recombination processes, especially in the alkali halides.

In the work to be described here, the three techniques mentioned above and a less well known one, Thermally Stimulated Charge Emission (TSCE) are applied together in order to understand electrical and optical processes in the material Potassium Magnesium Fluoride, $KMgF_3$.

In the present work the modus operandi is the following: Initially experiments were carried out to understand, as far as possible, the mechanism of the TSL. From this knowledge, an attempt was made to construct a preliminary model for the TSCE. The work was carried out in this order since experiments on TSL are easier to do and a greater variety of them appeared possible. Auxiliary information was obtained from standard optical absorption and electron paramagnetic resonance experiments.

Chapter II describes the material studied--$KMgF_3$, the processes of thermally stimulated luminescence and exo-electron emission, past work on these topics, and the present work. Some theoretical considerations of trapping and recombination are treated. Elements of the theory of resonant transfer of energy, which occurs in sensitization of luminescence, are given. This may be the mechanism operating in manganese-doped $KMgF_3$. Chapter III describes the experimental techniques and equipment used. In Chapter IV the various kinds of experiments performed and the resulting data are presented. In Chapter V the conclusions are given and a model is proposed to explain certain aspects of the thermoluminescence. Suggestions for further study are given.

CHAPTER II

BACKGROUND IDEAS AND PREVIOUS WORK

A. Potassium Magnesium Fluoride

Potassium magnesium fluoride, $KMgF_3$, is an insulator with the cubic perovskite structure (4). Figure 1 shows two unit cells of $KMgF_3$. The band gap is about 11 eV (5). Like the alkali halides, unirradiated $KMgF_3$ is transparent from the far ultraviolet to the far infrared.

When irradiated by electrons or gamma-rays, F centers are formed (6). The F center in $KMgF_3$ consists of an electron trapped at a fluoride ion vacancy and gives rise to the observed 275 nm optical absorption. F_2 (M) and F_3 (R) centers are also formed in the irradiation process. The F_3 center consists of three adjacent F centers (7,8) in the form of an equilateral triangle (Figure 2). The dose rate for the ^{60}Co source used in the present work is about 1.8×10^{13} MeV/cm^3 sec (5). The number of F centers formed may be estimated by Smakula's formula (9). A value of about 10^{16} F centers per cm^3 is typically obtained for several hours gamma irradiation.

If the material is irradiated with gamma rays or electrons at sufficiently low temperatures, stable V_K centers are formed. The first step in the formation of this defect is the loss of an electron from a normal fluoride ion (4). The resulting electrostatic forces cause a neighboring anion to move closer, thus trapping a hole at the site. This is equivalent to a self-trapped hole.

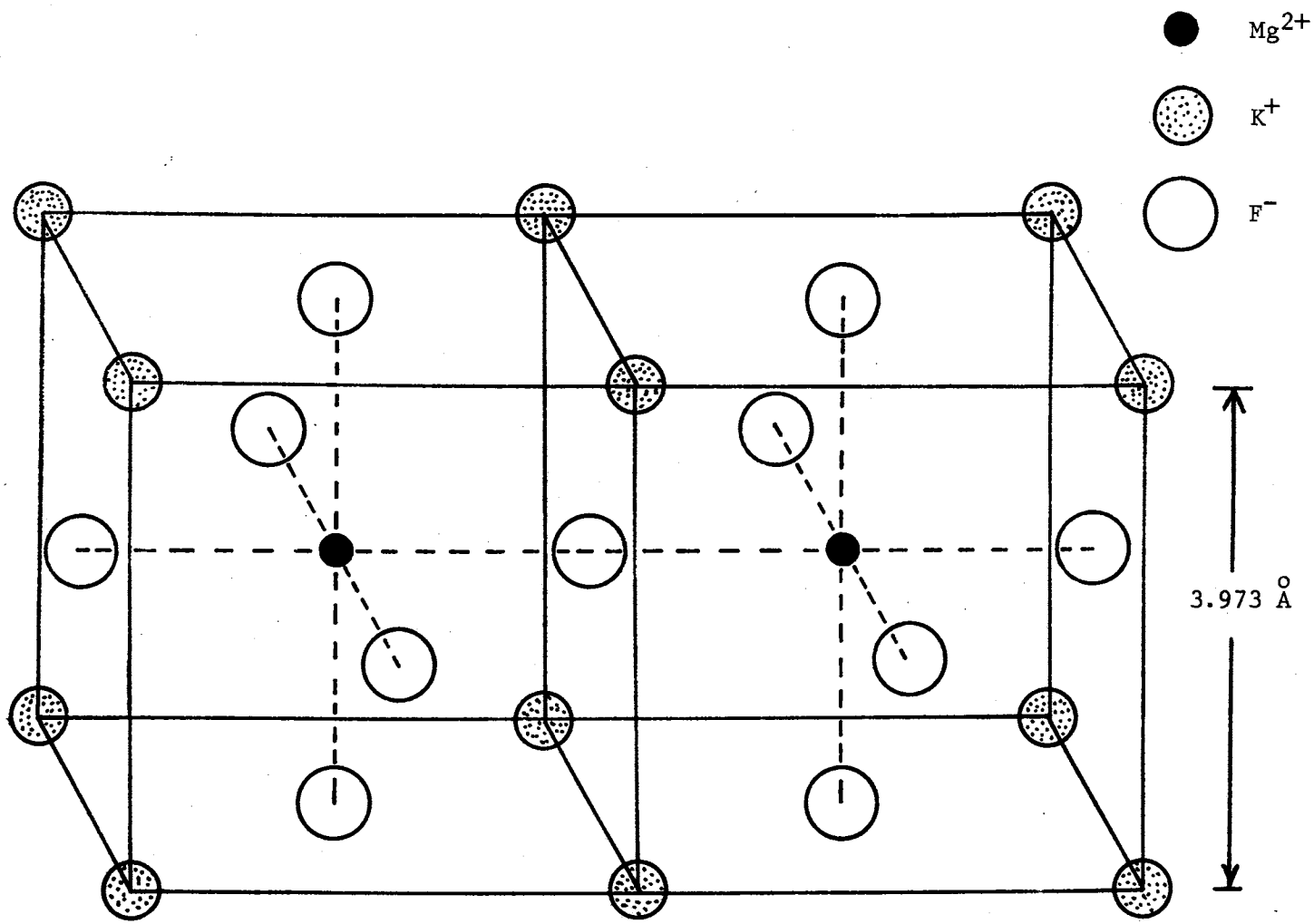

Figure 1. Two Unit Cells of $KMgF_3$

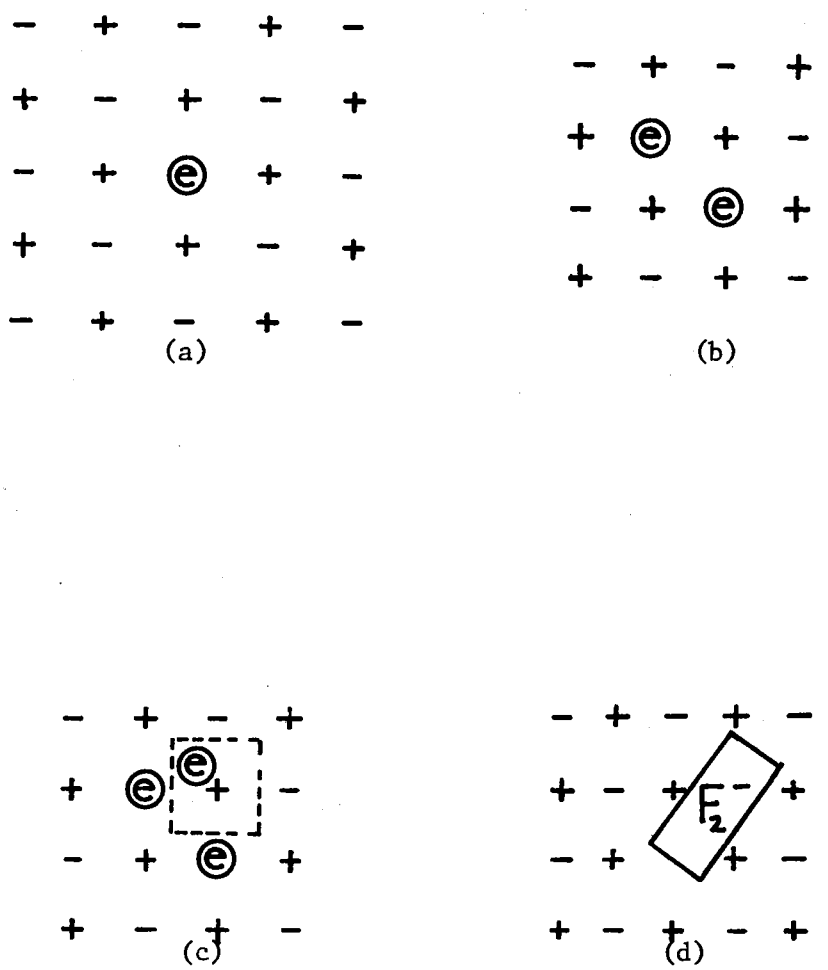

Figure 2. Configuration of the Color Centers: (a) F Center, (b) F_2 Center, (c) F_3 Center, (d) V_K Center

In general the radiation damage process is believed to follow the Pooley-Hersh mechanism (10, 11). In this scheme, a photon excites a halide ion:

$$X^- + h\nu \longrightarrow X^{-*}$$

This in turn can combine with another halide ion forming an excited halogen molecule ion:

$$X^{-*} + X^- \longrightarrow X_2^{=*}$$

The $X_2^{=*}$ can then dissociate into an atomic halogen which moves to an interstitial position leaving behind a vacancy (shown by $\square$), a normal halide ion, and an electron:

$$X_2^{=*} \longrightarrow X_{int} + \square + X^- + e^-$$

If this electron is trapped at a halide ion vacancy, an F center is formed. Of the several fates possible for the $X_2^{=*}$ molecule, one can lead to the formation of a V_K center:

$$X_2^{=*} \longrightarrow X_2^- + e^-$$

B. Thermally Stimulated Luminescence

Thermally Stimulated Luminescence (TSL) or thermoluminescence is a common technique for investigating certain aspects of defects in solids. Many materials, when irradiated at or below room temperature by ionizing radiation, undergo a redistribution of charge which results in the trapping of electrons and holes at defects; these may be visualized as providing localized levels in the forbidden energy band. When the material is subsequently heated, these trapped charge carriers may make radiative transitions to luminescence centers within the gap, emitting photons. Transitions can take place either directly or via the conduction band. If the intensity of the emitted radiation is plotted

against the temperature (a "glow curve"), peaks are obtained. In principle, one may calculate activation energies of the defects, measured from the bottom of the conduction band. However, approximations are made since the activation energy depends on other parameters such as the fraction of filled traps, heating rate, as well as the temperature, and the number of trapped charges. The spectral distribution of the emitted radiation may be obtained using emission spectroscopy apparatus. This gives information concerning the location of the luminescence centers below the conduction band edge if the transition is directly from the conduction band. In many cases, however, excited states complicate this simple picture.

An electron in a trap can be regarded as being in a potential well (12) with an associated activation energy E and frequency factor S. For no retrapping, S is the "attempt to escape" frequency of the trapped electrons or holes. The value of S is usually in the range 10^8 - 10^{12} per sec. There are many analyses employing different models, all designed to compute these and sometimes other trapping parameters. A simple method often used is the "initial rise" method (13). This method is probably the simplest to use but not always the most accurate (14).

Nicholas and Woods (15) have given a critical review of the methods using the maximum temperature and half width (16-21), the method using the variation of the heating rate (18-24) and the initial rise method. Later reviews are given by Braunlich (25) in 1966 and by Saunders (26) in 1969. A method worthy of attention is that due to De Muer (27). He takes account of the cross sections for trapping and retrapping and gives a graphical method for computing activation energy, frequency factor, and degree of retrapping. The limited value of all phenomeno-

logical models is pointed out in a recent paper (28). Activation energy calculations involve many parameters, some of which are uncertain so that analyses can be meaningful only when the defect structure of the solid is known. The "initial rise" method is probably most useful for values of activation energy which might be obtained by different workers.

C. Thermally Stimulated Charge Emission

A sensitive but less common method for probing defects in solids is by studying their exo-electron emission, first discovered by Kramer (29). The technique is often designated as Thermally Stimulated Exoelectron Emission (TSEE). To consider the generalized possibility of positive charge emission, we shall here refer to Thermally Stimulated Charge Emission (TSCE).

As in TSL, the processes occurring involve electrons and/or ions thermally emitted from traps located either in the bulk or at the surface. This is a "cold emission" since it can occur at very low temperature and has also been observed to have a peak structure. Since first observed in GM counters, TSCE has been attributed to be due to many processes: mechanical deformation, irradiation, phase changes, surface adsorption reactions (30), and chemical reactions (31, 32).

TSCE curves are plotted as counts/sec or current vs. temperature. As in TSL, TSCE peaks are obtained at characteristic temperatures and from these may be computed activation energies, which have the same limited validity. A TSL peak may coincide in temperature with a TSCE peak since the same defect may be responsible for both processes. In contrast to TSL, which is a bulk effect, TSCE probably arises from a thin surface layer of the material. Exo-electron emission is possible

also by optical stimulation (OSEE), using ultraviolet or visible light, depending on the trap depth (33). Two types of OSEE are distinguishable and different mechanisms have been proposed (34).

The energy distribution of exo-electrons may be measured using a retarding field technique (35). Electrons are usually emitted, but from ZnO and in the dehydration of $CuSO_4.5H_2O$ ions have been reported (36). A recurring question in TSCE work is: Where do the exo-electrons get their energy? One explanation is that high energy electrons in the "Maxwell" tail of the free electron distribution do have energy to escape. Since there is a greater number of more energetic electrons at higher temperatures, this theory would be more applicable in that region.

The Auger recombination mechanism is capable of explaining low temperature peaks (37). An example of this in an insulator is the thermal excitation of a bound hole which then recombines with a negatively charged center, transfer of this energy to another electron in the same or neighboring center, with subsequent ejection of this electron (Figure 3).

Various other factors, such as disturbances in the work function, potentials between surface and deeper layers, and direct emission from traps without involving the conduction band, are also invoked to explain how the electrons leave a material with high efficiency and energy. TSCE has been investigated in many materials, especially in the alkali halides, alkaline earth halides, and metal oxides. In this laboratory, Mollenkopf (38) has conducted a study of TSL and TSCE in MgO. Brotzen (39) reviews the work done on metals, oxide layers, and the effects in ultra high vacuum. Bohun (40) discusses the different mechanisms of TSCE in ionic crystals.

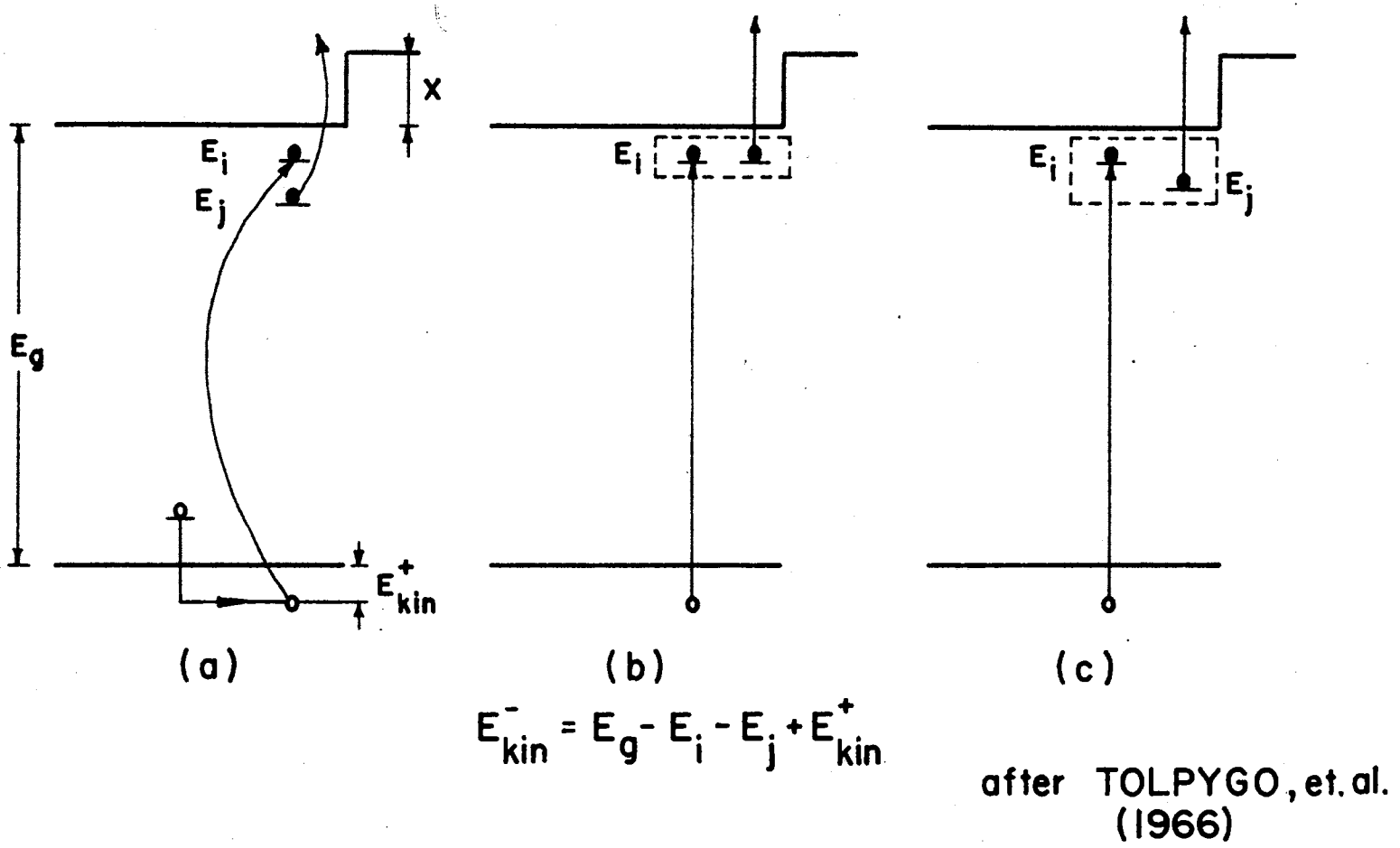

Figure 3. Auger Recombination Mechanism of a Hole (a) With an Electron of a Doubly Occupied Center, (b) With an Electron of a Neighboring Similar Center, and (c) With an Electron of a Neighboring Deep Center

As expected, peaks obtained in a given material vary with impurities, thermal history, surface structure, type of irradiation, etc. Becker (41), in his review article, discusses these and other factors in more detail. He also describes various types of apparatus and points out how this can affect the data. Becker also outlines applications of TSCE. Methods used to compute activation energies of TSL peaks have also been used on TSCE peaks. The method of Balarin and Zetzsche (42) is often used specifically for TSCE peaks.

In general, when a material is irradiated and warmed, the processes TSL, TSCE, as well as Thermally Stimulated Conductivity (which has not been included in this study) can result. Agreement between TSL and TSCE is not necessarily observed since:

(a) an electron may be ejected in a non-radiative transition (no TSL)

(b) an electron trap may be wholly within the bulk of the material (no TSCE)

(c) an electron trap on the surface may produce only TSCE.

Kelly (43), in his phenomenological theory, finds that TSCE has a sizeable effect on the other two effects, especially in thin films.

D. Previous Work by Others on $KMgF_3$

Some work has been done on the thermoluminescence of potassium magnesium fluoride (6, 44, 45). A literature survey indicates that there have been no charge emission studies made, except for the preliminary work by Mollenkopf (38) in this laboratory. As part of a wider study of color centers in $KMgF_3$ and $KMnF_3$, Riley (44) observed TSL from 7 to 300 K in $KMgF_3$, electron-irradiated at 7° (Figure 4). From thermally

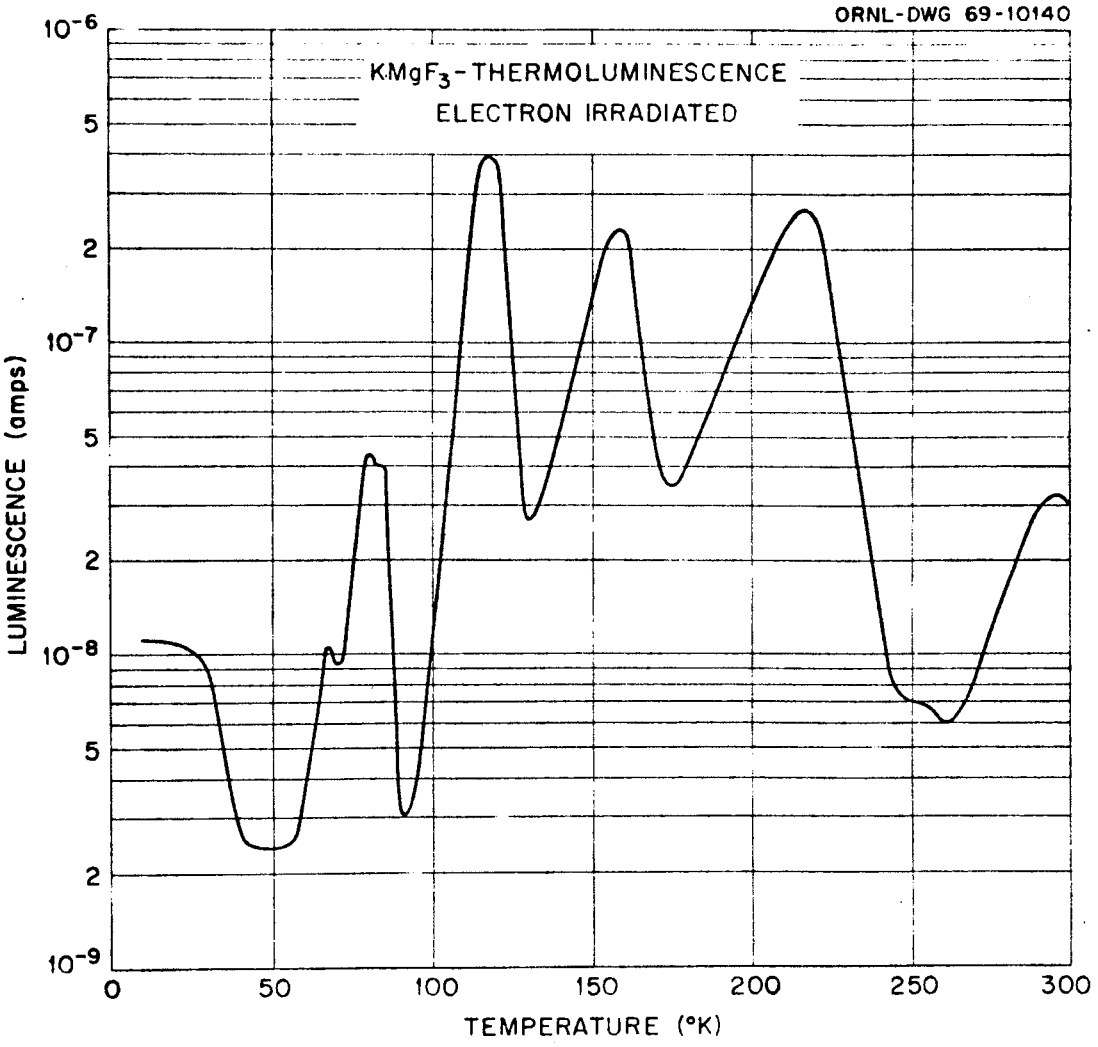

Figure 4. Thermoluminescence in $KMgF_3$ Gamma Irradiated at 7K (44)

annealing studies, he concluded that the glow peaks at 120 and 160 K are related to annealing stages of the V_K center and that the 215 K peak corresponds to an annealing stage of the F center. From his data on the spectral distribution of the glow peaks, he suggests that the 600 nm emission is due to Mn^{2+} impurity in the as-grown crystal. Later work (46) supports this last statement.

Altshuler and co-workers (45) obtained four TSL peaks from 100 to 300 K in pure and rare earth (RE)-doped $KMgF_3$. They conclude that the RE^{3+} ion (substituting for the Mg^{2+}) first captures an electron in the irradiation process. Then the thermally liberated V_K center approaches the ion, recombining with the trapped electron, producing luminescence characteristic of the ion. They attribute the different peaks as being due to different defects (impurity, dislocation, etc.) perturbing the RE ion.

E. Additional Considerations on Thermoluminescence Mechanism

In a study of thermoluminescence of CaF_2 X-irradiated at 77 K, Merz and Pershan (3) ascribe the 330 K peak to the diffusion of interstitial fluorine atoms through the lattice. For this process they estimate an activation energy in the range of 0.9 - 1.2 eV.

Altshuler and co-workers base their interpretation of the low temperature TSL behavior in $KMgF_3$ on the ideas of Merz and Pershan (3), who investigated TSL in pure and rare earth doped CaF_2. They found glow peak temperatures to be independent of the doping, implying an association with V_K centers in common with all the RE ions. They explain their 330 K glow peak as due to diffusion of interstitial fluorine atoms (F^o)

through the lattice. This is in contrast to the low temperature hole diffusion, a motion requiring less energy. Thus the 330 K glow peak activation energy would be a measure of the energy to free an F^o for diffusion through the CaF_2 lattice. No details are given on the recombination process.

A similar mechanism is cited by Ausin and Alvarez Rivas (47). In their study of TSL and F center annealing in room temperature gamma-irradiated KCl, they find:

1. An annealing step in the F center optical absorption for each TSL peak, and
2. The area under the TSL curve is proportional to the concentration of F centers measured before heating.

These authors state that the idea of the F centers acting as traps for electrons or recombination centers for holes does not explain the observed data. Their model is that interstitial chlorine atoms become mobile as the temperature is raised and recombine with F centers, with the electron-hole recombination emitting the same luminescence for each of the TSL peaks. This model explains the vanishing of peaks I, II, III as being due to aggregation of interstitials at high F center concentration. In their calculations of frequency factors using various methods, they get abnormally large values; this again casts doubt on the idea of F centers acting as electron traps.

The kinetic model of the annealing of defects is based on that due to Damask and Dienes (48). The time rate of change of defect concentration n is given by:

$$\frac{dn}{dt} = K_o \exp\left(\frac{-E}{kT}\right) n^{\delta}$$

where K_o is the pre-exponential factor and δ is the kinetic order.

There is an analogy here with the usual equations of thermoluminescence (δ = 1,2); however, the physical meaning is different: E is the activation energy of the process rather than the trap depth, while S and S' correspond to K_o. In a simple case, the intensity of recombination is expected to increase with concentration of diffusing centers and with the concentration of recombination centers.

A recurring problem in the thermoluminescence and radiation damage of alkali halides is the role of F centers. Some (49, 50) claim that the growth of F centers can be divided into two or more stages, these being due to the anion vacancies present in the crystal before irradiation and those created in the radiation damage process itself. Thus attempts are made to connect certain above room temperature glow peaks with observed F center annealing stages. Others (51) find no connection, although both effects occur in the same temperature range. To summarize, the following topics were discussed: the mechanism of the low temperature TSL in CaF_2, the role of manganese in the recombination process, and the connection if any between the F center annealing and the TSL above room temperature. It was felt that these questions required consideration in the case of $KMgF_3$:Mn.

F. Elements of the Theory of Sensitized Luminescence

Many phosphors incorporate manganese as the luminescent ion since it exhibits visible emission in a wide variety of host lattices. An important problem here is the mechanism of the luminescence and the transfer of energy in these phosphors. According to Goldberg (52) there are four known mechanisms for the transport of excitation energy

in inorganic solids: radiative transfer, charge transport mechanism, exciton mechanism, and resonance transfer. The last named best describes the situation in many of the manganese-doped phosphors (53).

When phosphors containing impurities for visible emission have no absorption bands in the region 200-400nm, it is impossible to excite them with UV. Often, however, a second impurity can be introduced in the above spectral region and usually having its own fluorescence emission at longer wavelengths. Thus the sensitizer will give rise to emission from the activator or emitter. A well studied example is ZnS: Pb: Mn, the sensitizer being Pb (54). The sensitization effect is important in practice, also, since in most fluorescent lamp phosphors it affects the efficient conversion of energy from the 254nm radiation of the low pressure mercury discharge into visible radiation of suitable spectral content.

A review of the different theories has been given by Botden (55), and Dexter (56) has given the quantum mechanical resonance theory. This mechanism may operate in Mn doped $KMgF_3$.

The transfer of energy between ions in a crystal may be accomplished in two possible ways without the transfer of charge:

1. A "cascade" mechanism which is a radiative transfer of energy through the emission and reabsorption of photons.
2. Long range resonant interaction (LRRI, also called Forster-Dexter interaction). Here an ion which has absorbed a photon interacts via a multipole-multipole or exchange interaction with another ion and subsequently transfers the excitation. It is this mechanism that is believed to operate in many of the manganese-activated phosphors.

We will now consider the process of sensitization of luminescence in KCl: Pb: Mn (54). Here the Mn^{2+} is called the activator (A) and has no appreciable absorption band in the UV or visible spectrum. The Pb, which is the sensitizer (S) can absorb in this region and transfers radiation of longer wavelength to the Mn^{2+}, which then emits its characteristic radiation.

The entire transfer process consists of five stages:

1. Absorption of a photon of energy E_o by the sensitizer,
2. Relaxation of the lattice surrounding the sensitizer by an amount such that the available electronic energy in a radiative transition from the sensitizer is $E_1 < E_o$,
3. Transfer of energy E_1 to the activator,
4. Relaxation around the activator such that the available electronic energy in a radiative transition is $E_2 < E_1$,
5. Relaxation around the sensitizer to a state similar (but not necessarily identical) to its original unexcited state,
6. Emission of energy E_2.

The energy transfer is regarded as a quantum mechanical resonant process. The difference in the energies E_o and E_1 corresponds to Stokes's shift of wavelength.

Dexter calculates a critical impurity concentration of 3×10^{-4} per cm^3 for appreciable S-A transfer to occur. For this concentration, S is able to sensitize 2,900 sites in NaCl, an ionic crystal with an interatomic spacing similar to $KMgF_3$. A literature survey indicates fair agreement of the theory with experiment from the meager data available.

G. Scope and Method of Study

In the low temperature region, doped and undoped samples of $KMgF_3$ were irradiated with electrons, gamma rays, or ultraviolet radiation. One purpose of these experiments was to study the creation and filling of the low temperature traps. This helped to see if a different mechanism operated here compared to the above room temperature region.

These experiments and relevant EPR experiments help (1) to identify the traps created by UV at the low temperature and (2) the connection between their recombination (as the temperature is increased) and valence changes in manganese or other impurities.

In the above room temperature region, the following experiments were carried out.

(1) Effect of gamma ray and UV irradiations. The objective here was to see if the gamma rays create the traps and if UV fills them as usually occurs in the alkali halides.

(2) Effect of gamma ray dose on the concentration of F centers and on the TSL peak spectrum. This is to see if certain TSL peaks grew preferentially with gamma ray irradiation time.

(3) Correlation of thermal annealing of F centers and optical absorption changes. This may be additional evidence for relating F center concentration changes and TSL peaks.

(4) Effect of F band illumination upon the glow peak structure. To observe which TSL peaks have a positive correlation with F centers and which have a negative correlation.

(5) Spectral composition of the glow peaks. To see if different luminescent centers are associated with each TSL peak.

(6) EPR experiments to detect valence changes in impurities, particularly manganese. To observe any concomitant changes in hole centers (if present) or F center concentrations.

From the information obtained above it is hoped to make a model of the thermoluminescence process. In particular the role of V_K centers, F centers, and manganese are of interest. In addition some understanding of the TSCE mechanism may be gained because of the similarity with the TSL peak spectrum.

CHAPTER III

EXPERIMENTAL EQUIPMENT

A. Samples

Several undoped and two manganese doped samples of $KMgF_3$ were used. They were grown by Riley (3) at Oak Ridge National Laboratory; this reference also gives the impurity analyses.

For TSL and TSCE measurements, samples with as-grown faces were used where possible. In fact, little difference in data was observed between these and polished samples. For optical absorption measurements, samples were cut with approximately parallel sides using a Metals Research Ltd. diamond saw. The samples were then polished with a Syntron lapper-polisher using Linde A 0.3μm α-Al_2O_3. After repeated TSL and TSCE runs, the sample surface that was used showed some deterioration and was repolished slightly in order to obtain consistent optical absorption measurements. This surface deterioration did not alter the reproducibility of TSL runs. Of course, even very slight surface changes affected the TSCE. But reproducibility of the TSCE was found difficult to achieve even with the greatest precautions.

Prior to any measurement, samples were washed in acetone in an ultrasonic cleaner. More elaborate cleaning prior to TSL and TSCE runs did not produce significant differences.

Samples were irradiated with ^{60}Co gamma-rays and then kept in darkness prior to measurement. The typical dose rate was 1.8×10^{13}

MeV/cm^3 sec (2). For some experiments samples were also irradiated by 1.5 MeV electrons from a Van de Graaff accelerator. The UV light source was a Cenco Hg light, Model 87298.

B. The Combined TSL and TSCE Apparatus

The sample is mounted on the bottom of a cold-hot finger which also permits cooling of the sample to near liquid nitrogen temperature (Figure 5). The sapphire viewport underneath permits irradiation by ultraviolet light and luminescence detection by photomultiplier tube. The detector for charge emission is attached to the front of the apparatus as are copper-constantan thermocouple leads.

The charge emission detector is a gas flow counter (Geiger-type). It has its central anode at -1000 volts, which is provided by a Hamner Model N-4035 power supply. The exo-electrons are detected indirectly by the positive ions which are formed in equal numbers. These ions travel to the outer cylinder, which is connected to a Model 610B Keithley Electrometer. Thus is the charge emission measured. More detail on the gas flow counter is available in the thesis by Mollenkopf (38). The electrometer output is fed into the Y axis of an XY recorder (Omnigraphic Model HR-96), operated in the "time" mode.

A 1P28 photomultiplier tube (S-5 response) operated at -850 volts, with an associated voltage divider network, detects the luminescence. The output of the photomultiplier tube is fed into a 602 solid state Keithley Electrometer. The Y axis of a Moseley 135 XY Recorder graphs this output while the X axis indicates the sample thermocouple voltage.

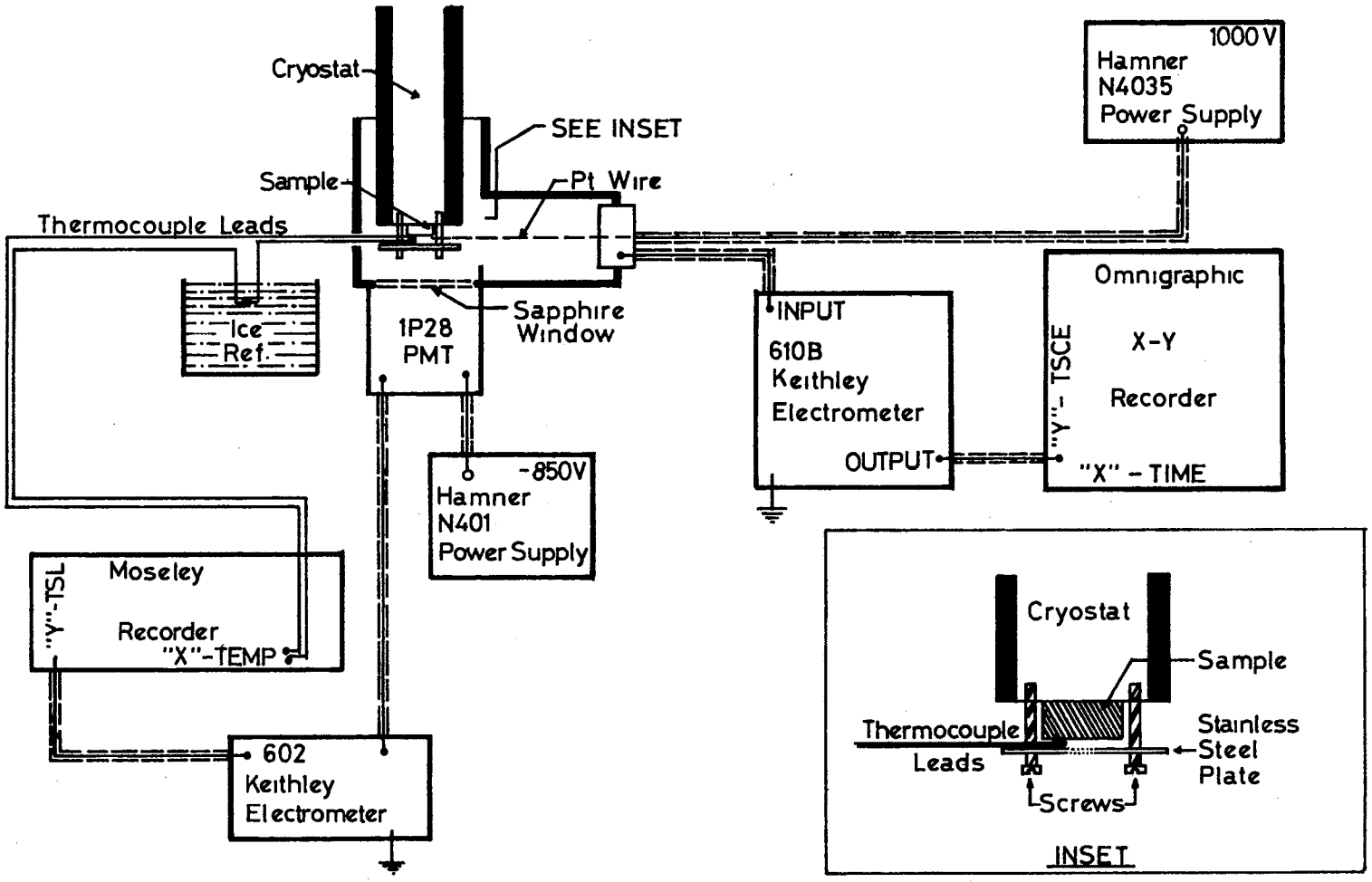

Figure 5. Block Diagram of Simultaneous TSL and TSCE Data Recording System

In a typical experiment, a sample which has been gamma-irradiated is mounted. The system is pressurized to about 7 cm Hg with a 90 percent Argon--10 percent Methane counting gas. The gas pressure is measured with a manometer containing n-butyl phthalate, a low vapor pressure oil, before and after charge emission. An Edwards high vacuum variable leak controls gas flow to within 0.05 cm Hg on the average.

Starting from room temperature, the sample is heated rheostatically in a reproducible way, the TSL and TSCE being recorded simultaneously. To re-excite the low temperature peaks, the sample temperature is lowered to near 77 K. Then the sample is excited using unfiltered ultraviolet light from a Cenco mercury lamp, followed by heating. The heating rates below and above room temperature are about 0.3 K/sec and 0.15 K/sec respectively. Both heating rates are approximately linear.

C. Emission Spectroscopy Equipment

The sample is held on an aluminum slide which fits into the heating block (Figure 6). The heating rate was 0.06 K/sec and kept approximately linear by a motor driven rheostat. A copper constantan thermocouple is embedded in this block near the sample. The side of the sample is opposite the 1P28 photomultiplier tube. The large flat surface of the sample faces the monochromator. The Monochromator was a Bausch and Lomb 0.5 meter Model 33-86-40 with its wavelength drive connected to the X axis of a Moseley Model 7000A recorder. At the monochromator exit is a C31034 Photomultiplier tube (GaAs photocathode) operated at -1000 volts at room temperature by a Fluke Model 412A supply.

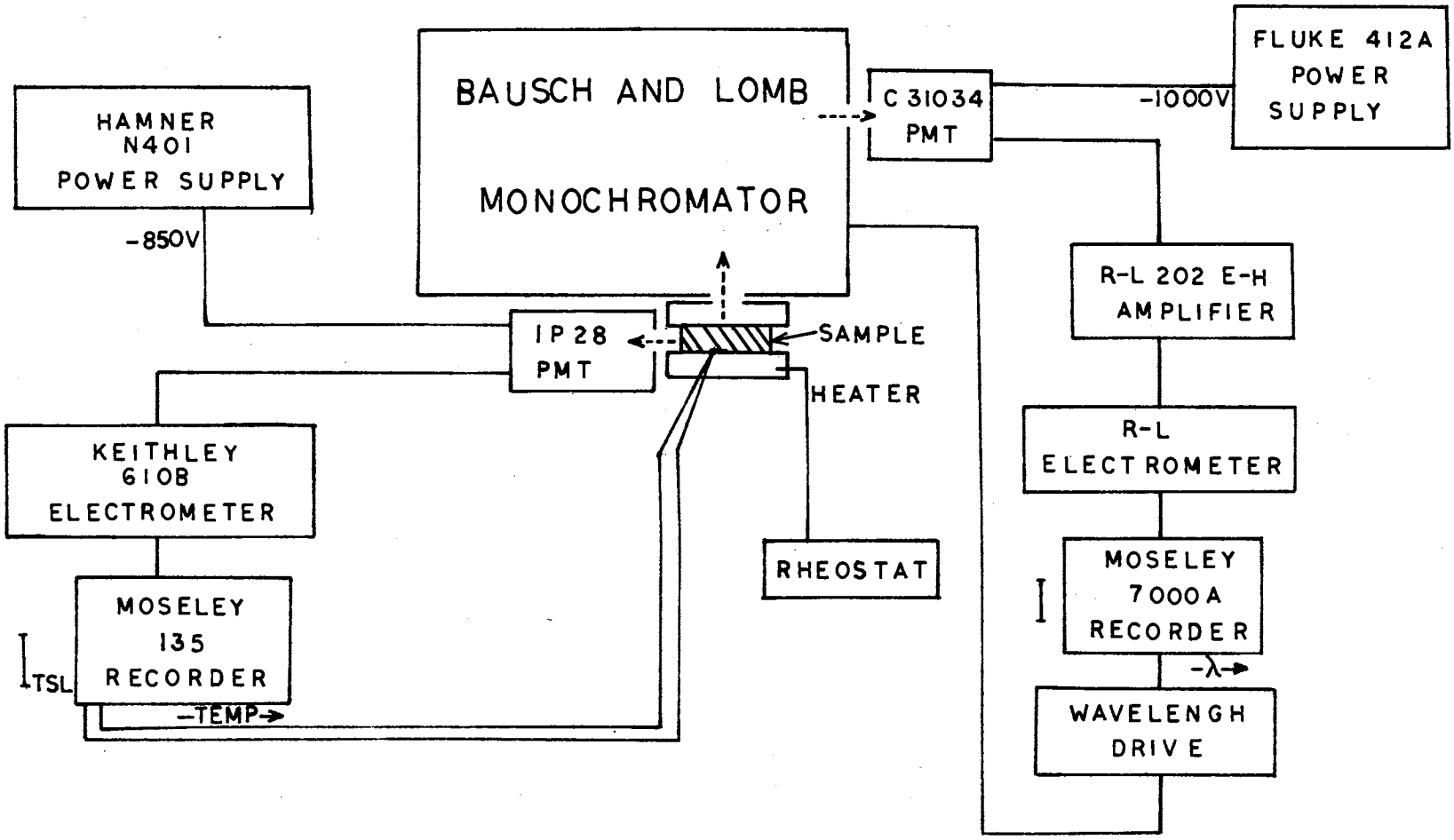

Figure 6. Block Diagram of Emission Spectroscopy Equipment

The output of the PMT was fed to a Model 202 E-H Research Labs Electrometer Amplifier and then to the Y axis of the Model 7000A recorder. Thus a plot of luminescence intensity versus wavelength is obtained. To measure the total spectral emission, the 1P28 output is connected to a 610B Keithley Electrometer and then to a Moseley Model 135 recorder. Typically, a wavelength scan from 300nm to 950nm is made through the maximum of a glow peak. Scans were made in increasing and in decreasing wavelength, and the mean was taken.

D. Optical Absorption Equipment

The existance of defects which absorb optically may be detected by a Spectrophotometer.

The Cary 14 Spectrophotometer is a double beam instrument and was used to measure the optical density (O.D.) of the samples. A peak in the O.D. versus wavelength graph means a certain type of center has its first excited state at that particular wavelength; e.g., 275nm (4.5 eV) for the F center in $KMgF_3$.

The optical density is defined as:

$$O.D. = \log_{10} (I_0/I)$$

where I_0 = Intensity of light beam entering sample and

I = Intensity of light beam leaving sample

It can be shown (9) that under certain conditions the concentration of centers is proportional to their optical density.

E. Electron Paramagnetic Resonance

The EPR technique can be very helpful for obtaining local information on defects in crystals. Thus valence changes of impurity ions can

be detected, which may help in making a model for the thermoluminescence.

The microwave system was an X-band homodyne type with 16KHz magnetic field modulation. A Varian V-4531 reflection cavity was used. Horizontal slots in the side of the cavity permitted excitation of the sample with light. The maximum sensitivity of the system was approximately 2×10^{12} spins/cm^3 at 77 K.

EPR runs at around 125 K to 570 K were effected by flowing nitrogen gas through stainless steel tubing submerged in liquid nitrogen. An alternative method was a variable temperature control heating element for both low and high temperatures. A copper constantan thermocouple near the sample monitored its temperature. Temperatures could be controlled to within 5-10 K permitting heating runs similar to the TSL experiments.

CHAPTER IV

EXPERIMENTS AND OBSERVATIONS

This chapter describes the various kinds of experiments that were performed in order to collect information about the role of F centers and possible valence changes in Mn^{2+} related to the thermoluminescence in $KMgF_3$. The various sections relating to these experiments are described as follow:

Effect of UV and Gamma Irradiation: Here are described the effect on TSL and TSCE of irradiating the sample at room temperature with gamma-rays and the LN temperature with UV.

Variation of Gamma-Ray Dose: These runs show the effect of varying the gamma-ray dose.

Emission Spectroscopy Experiments: These experiments show the spectral distribution of some of the TSL peaks and their re-excitation capability with UV light.

Illumination into the F Band: This series of experiments shows the effect of illuminating the sample with light of wavelength approximating the F center absorption wavelength (275 nm).

Thermal Annealing and Optical Absorption Correlation: This series of experiments shows the correlation between thermal annealing and optical density of the F centers.

EPR Experiments: These experiments describe attempts to detect Mn^{2+} valence changes and the possible formation of V_K centers produced by UV light at low temperatures.

A. Effect of UV and Gamma Ray Irradiations

In the following "Gamma Run" will refer to the result of first irradiating the samples with gamma rays (Figures 8, 11). The term "UV Run" will refer to the result of exciting a sample with UV after a "Gamma Run." Note that the peak temperature will vary a few degrees Kelvin in different runs.

1. Undoped Samples

First annealed samples were cooled to near 77 K and irradiated with UV light for two hours. No thermoluminescence resulted, but very small TSCE peaks at about 240, 340, and 452 K were produced (Figure 7). Then the sample was taken out of the system, gamma-irradiated for 50 minutes and remounted. The run (subsequently called a "Gamma Run") was started again from near 77 K so as to obtain a consistent heating rate. Sizeable TSL peaks appeared at about 342, 369, 415, 444, 476, and 523 K. Large TSCE peaks were observed at 340, 420, 450, and 570 K (Figure 8). In the next run, shown in Figure 9, the sample was irradiated with UV light for 1,000 seconds without removing it from the system. Low temperature TSL peaks occurred at 182 and 239 K, while TSCE peaks occurred at 186 and 241 K. These TSL and TSCE peaks occurred usually at almost the same temperature. Above 273 K, the TSL peaks of Figure 8 were present but very small. These re-excited peaks were also more separated than in the Gamma Run of Figure 8. In subsequent runs, the TSL peaks had decreased to practically zero, but the TSCE peaks had decreased only slightly (Figure 10).

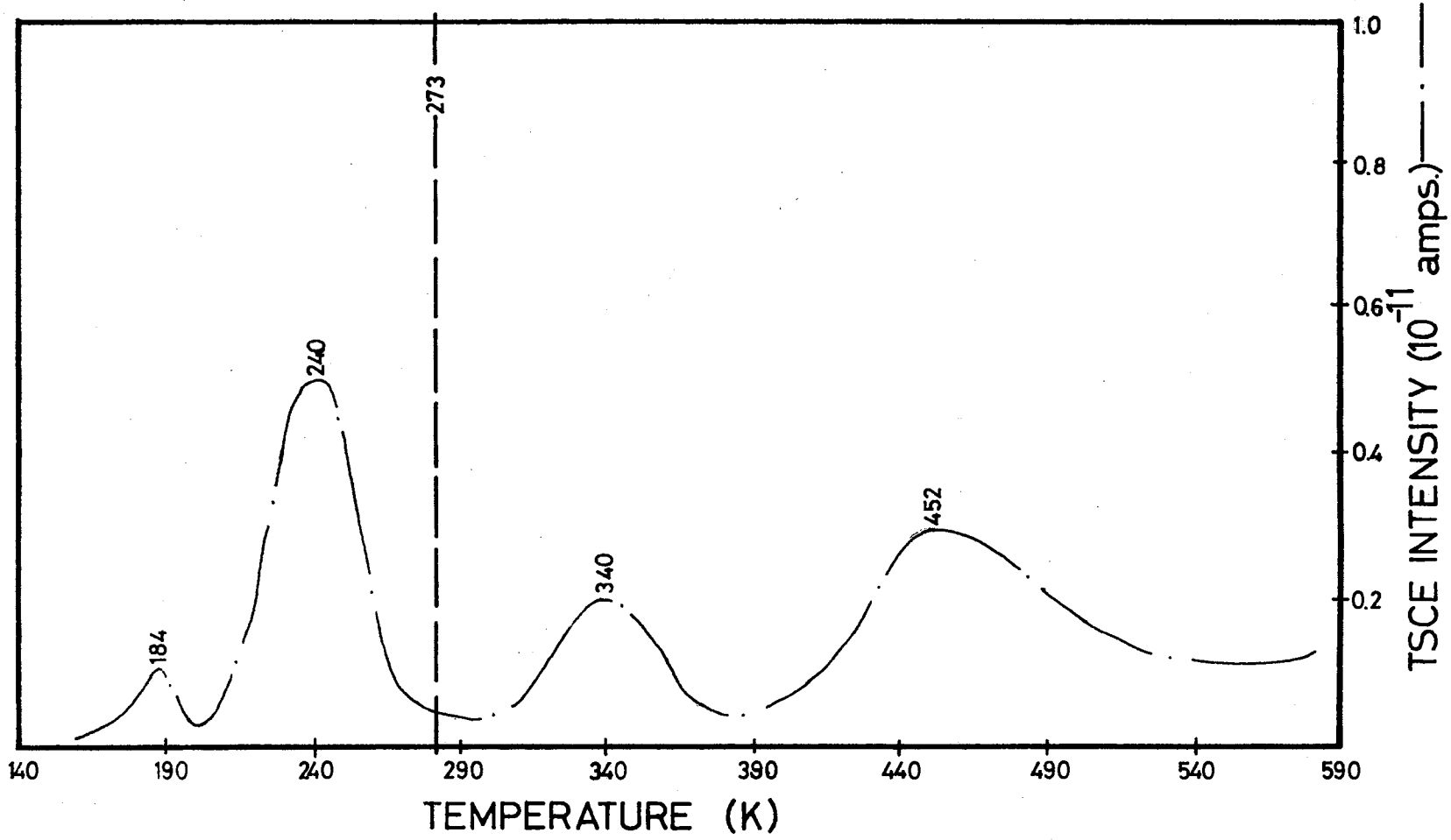

Figure 7. TSCE of Undoped $KMgF_3$ Irradiated by Unfiltered UV Light at LNT

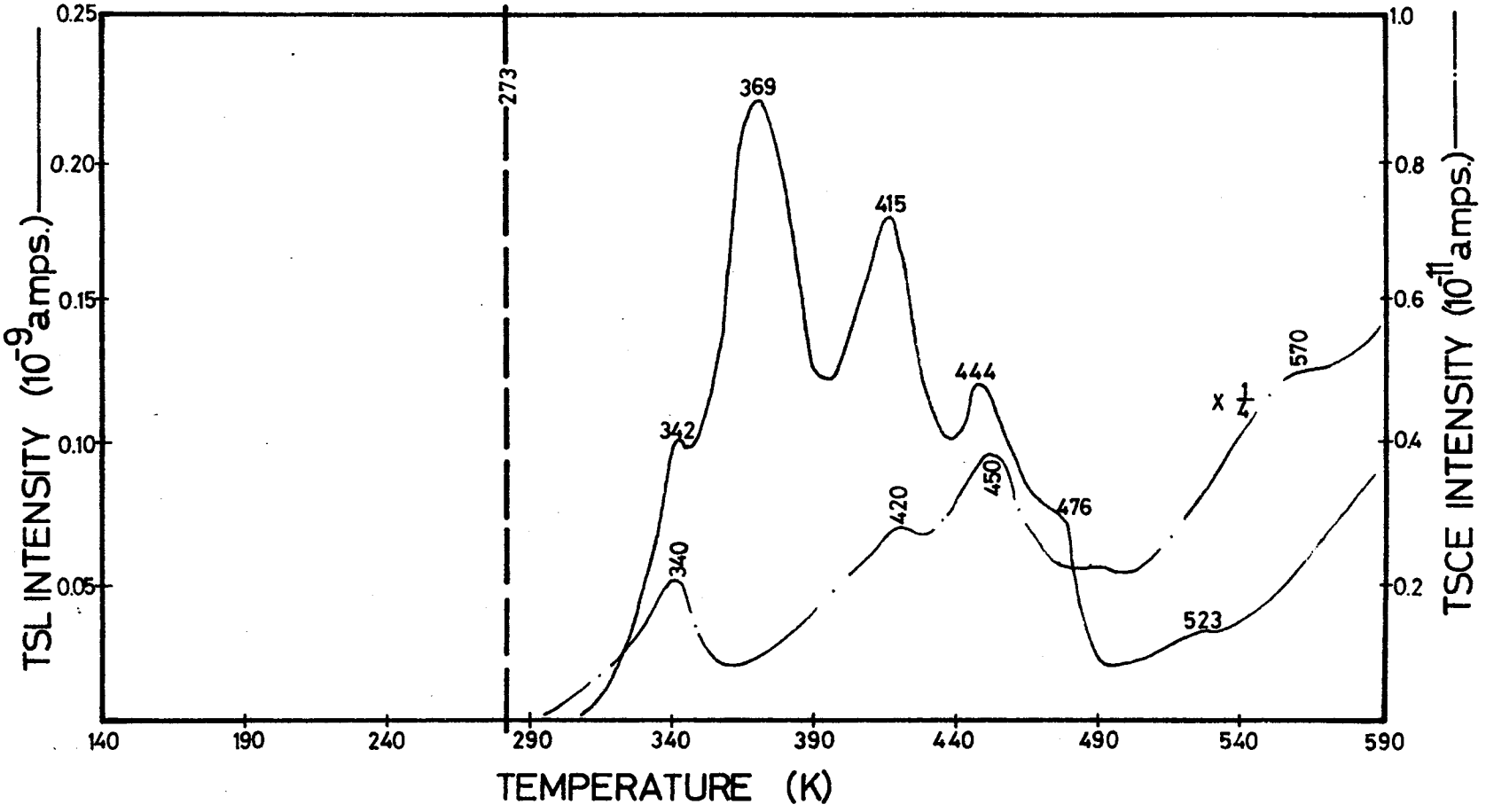

Figure 8. TSL and TSCE of Undoped $KMgF_3$ Irradiated at Room Temperature by Gamma Rays

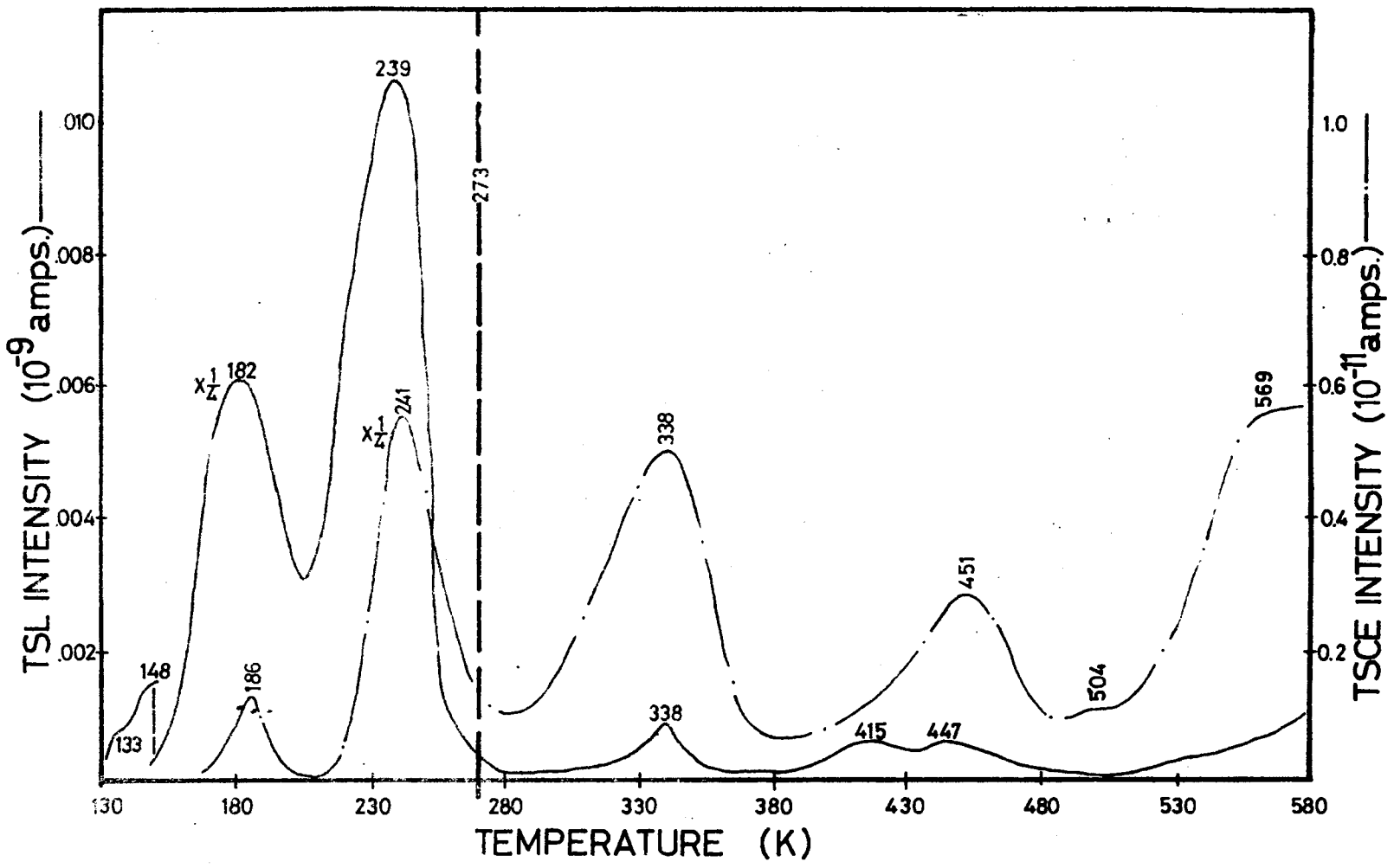

Figure 9. The Effect of Unfiltered UV Irradiation at LNT on the Undoped Crystal Subsequent to Run of Figure 8

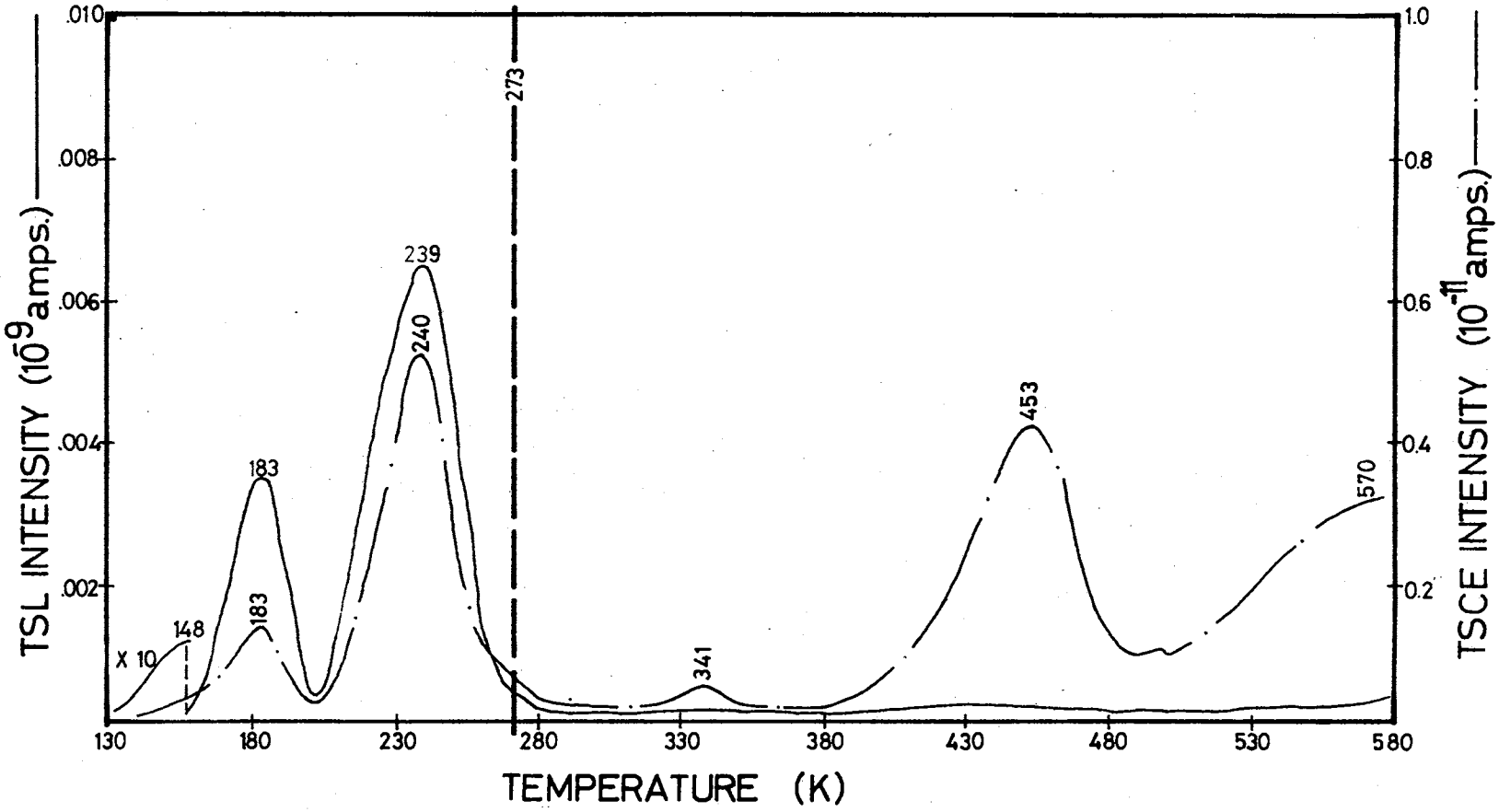

Figure 10. The Effect of an Additional UV Irradiation on the Undoped Crystal Subsequent to the Run of Figure 9

2. Doped Samples

The same sequence of experiments was carried out on the doped samples as on the undoped samples.

On irradiating annealed samples with UV light even for two hours, only one small TSCE peak at 330 K was produced. Again, as in the undoped samples, no TSL peaks appeared. When the sample was gamma-irradiated, very large TSL peaks appeared at 339, 408, 464, 540, and 574 K (Figure 11).

When the sample was re-excited with UV without removal from the system, low temperature TSL and TSCE peaks again appeared, and small, well-separated peaks above room temperature also appeared (Figure 12). It is seen that the 337 and 540 K peaks recur. All these peaks were re-excited in a subsequent run (Figure 13), except the 540 K peak, which is probably overshadowed by the increasing black body radiation.

3. TSL Summary

The TSL summary is as follows:

1. For both the undoped and doped samples, no TSL peaks are apparent after two hours UV excitation.
2. The heights of the peaks obtained by re-exciting the samples with UV after initial gamma-irradiation ("UV Run") are much smaller but more accentuated than those obtained in the Gamma Run.
3. For the undoped sample, each TSL peak (except the 370 and 570 K peaks) is present in the "Gamma Run" and in the "UV Run." In the doped sample the 290, 408, and 570 K peaks of the "Gamma Run" are not apparent in the following "UV Run."

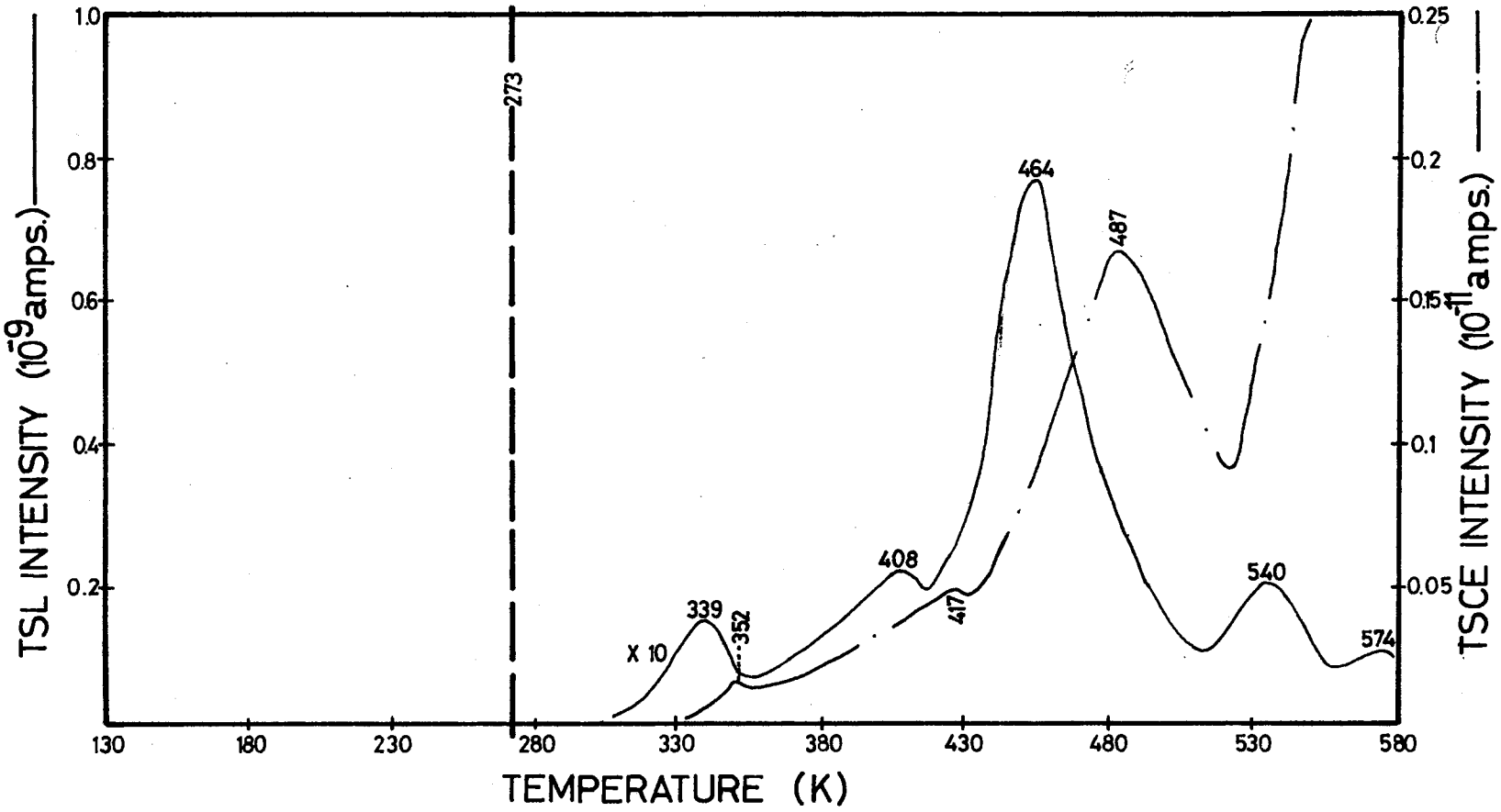

Figure 11. TSL-TSCE of Doped $KMgF_3$ Gamma Irradiated at Room Temperature

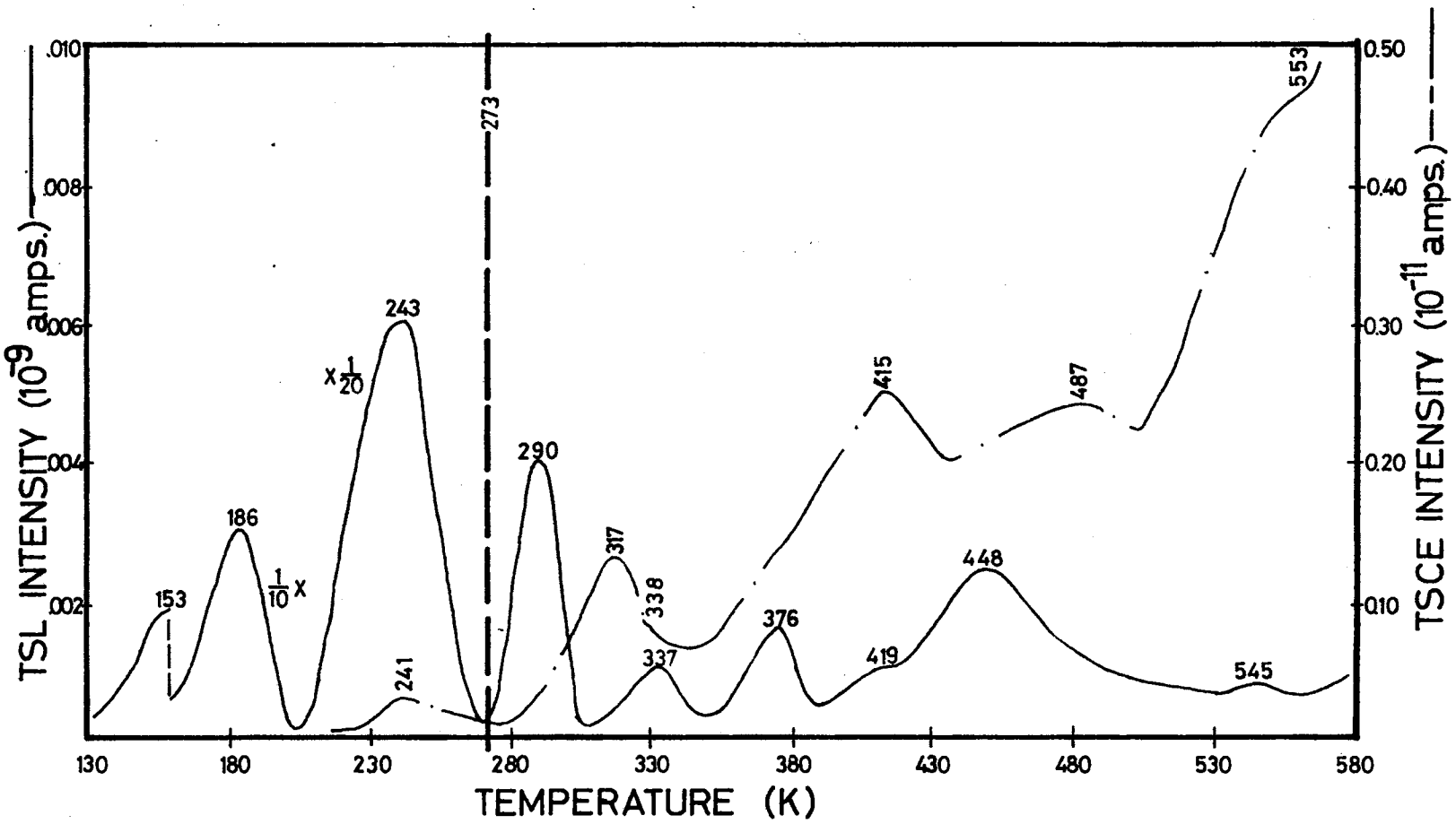

Figure 12. The Effect of an Unfiltered UV Irradiation at LNT on the Doped Crystal Subsequent to the Run of Figure 11

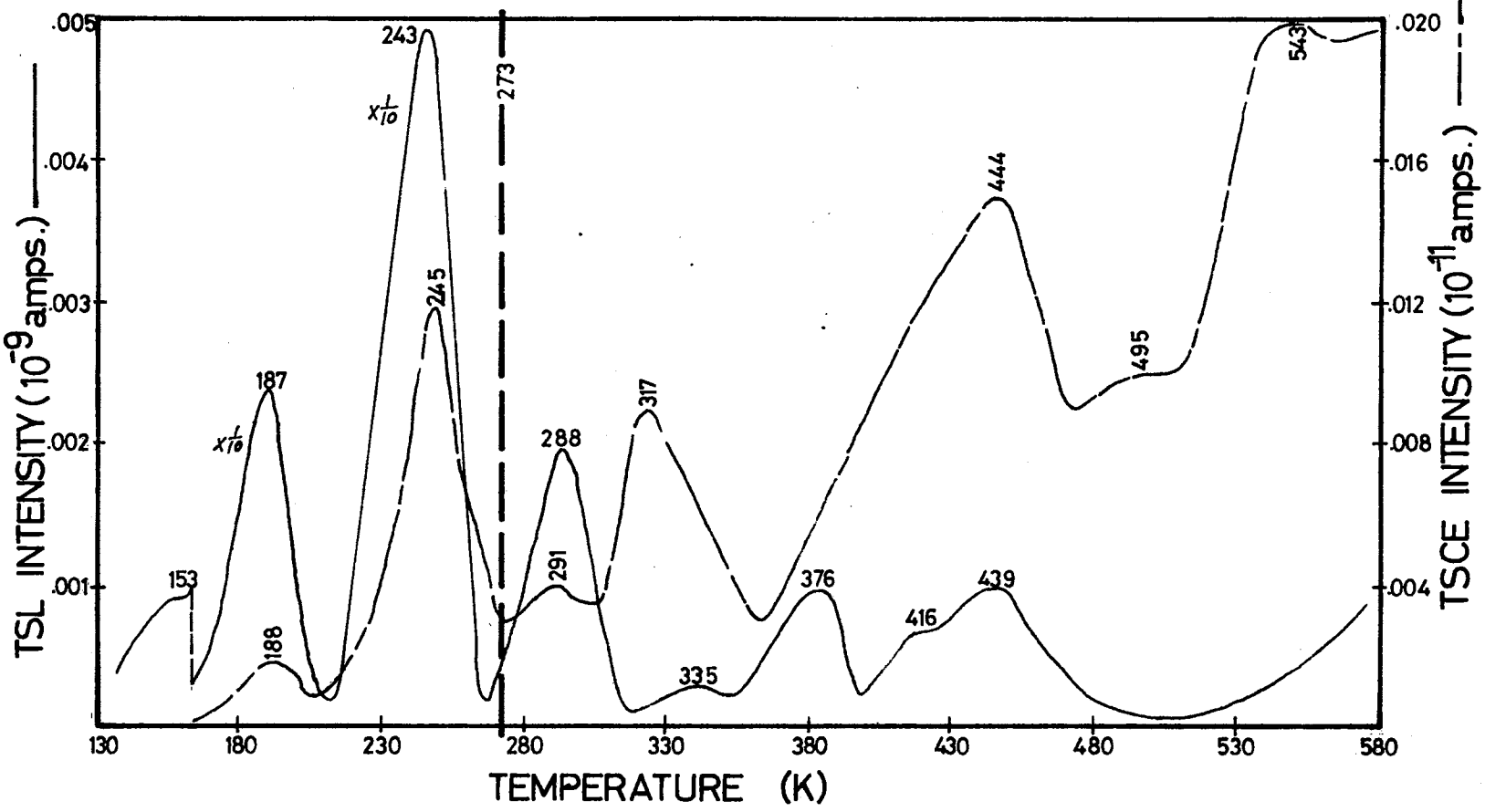

Figure 13. The Effect of an Additional UV Irradiation at LNT on the Doped Crystal Subsequent to the Run of Figure 12

4. For both samples TSL peaks at 150, 184, and 240 K are produced by UV at 77 K only after initial gamma-irradiation. The 184 and 240 K peaks are more consistent in height and temperature than the above-room temperature peaks.

4. TSCE Summary

The TSCE summary is as follows:

1. In both samples, one or more small peaks appeared after two hours UV excitation, and these were very much enhanced by gamma-irradiation.
2. In repeated UV Runs, all the peaks are capable of re-excitation in contrast to the TSL peaks, which die out within two UV Runs after the initial Gamma Run.
3. The levels of the TSCE peaks in the doped sample were generally lower than the TSL peaks in the doped sample whereas the opposite was true for the undoped samples.
4. In general, there is usually a TSCE peak corresponding to each TSL peak.

5. Summary

The data can be interpreted by saying that apparently the gamma-rays create and fill the traps and that the UV only fills them. It is apparent that the UV is not capable of creating the traps initially. Since gamma-rays also produce F centers, it is appropriate to ask what is the connection, if any, between them and the peaks of TSL and TSCE.

B. Variation of Dose

One indicator of how the TSL peak heights vary with F center concentration is to irradiate samples for various lengths of time and monitor the F center optical density. Thus thermoluminescence runs similar to those in Section A were carried out by simply varying the gamma ray irradiation time and monitoring the optical absorption before each TSL Run. In this way the variation of TSL peak height with F center optical density is investigated (Figures 14 and 15).

Figure 14 is a collection of the results typical of the undoped samples. This consists of the peak heights of each of the TSL peaks (where present) plotted against the irradiation time. In going from short to long irradiation times a peak tends to be "lost" or overshadowed, perhaps by the width of a higher temperature peak. Thus the 340 K peak is seen only as a shoulder in the three-hour Gamma Run. At longer irradiation times this peak seemed to occur at higher temperatures.

Figure 15 shows the data typical of the doped samples. The 440 and 460 K peaks of the doped samples are taken as corresponding to the 430 and 450 K peaks of the undoped samples, respectively. At very long gamma irradiations only the 420 and 540 K peaks are observed. The 340 and 460 K peaks are not observed for irradiation times longer than three hours.

A significant feature is that the TSL peak spectrum of a lightly irradiated doped sample has similar intensity levels as the TSL peak spectrum of a heavily irradiated undoped sample. This implies that the net TSL of all the samples increases with the F center concentration and with the manganese concentration. This means a joint probability of

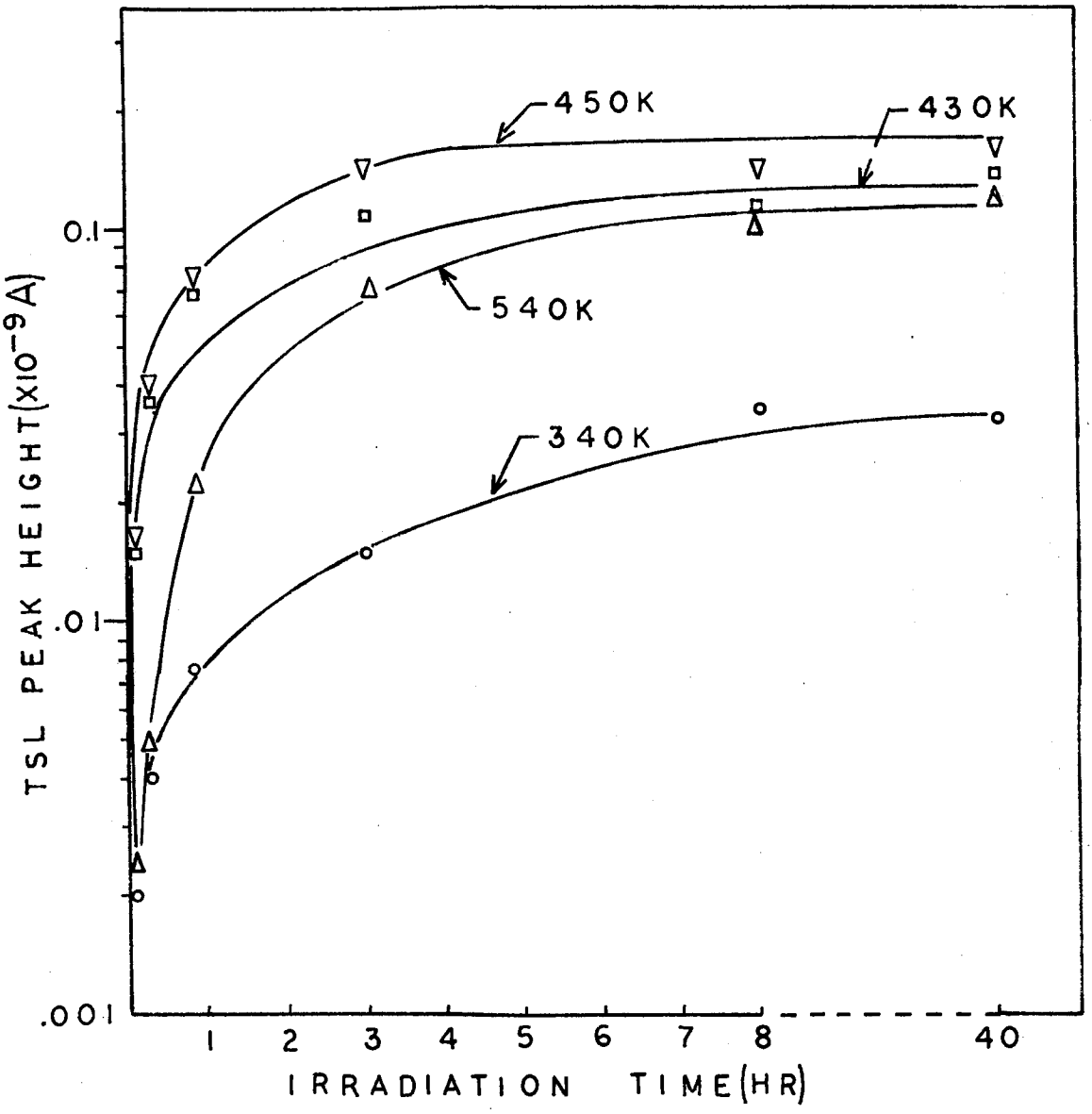

Figure 14. Variation of TSL Intensity With Gamma-Ray Irradiation Time for the Undoped Crystal

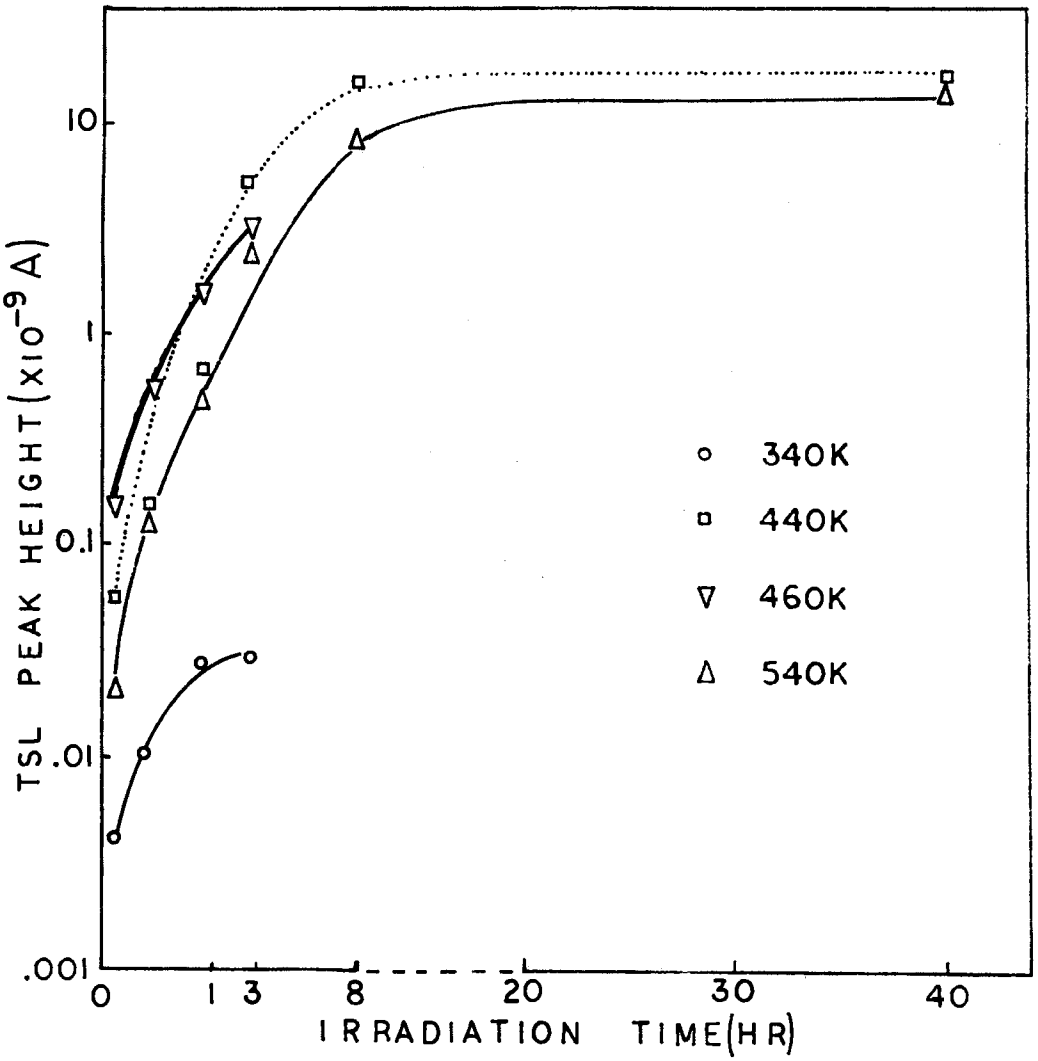

Figure 15. Variation of TSL Intensity With Gamma-Ray Irradiation Time for the Doped Crystal

recombination depending on these two concentrations, which will be discussed in the model outlined later.

For both the undoped and doped samples the general trend of the variation of the TSL peak height is the same. A rapid rise in peak height at short irradiation time and saturation at long irradiation time are observed. The saturation level for the doped sample is higher than in the undoped sample.

If the F center optical density is plotted against TSL peak height, similar trends are observed. Thus the first peak 360/340 K stops growing although the F center concentration still increases. Thus it is reasonable to say that this peak is not related to F centers.

C. Emission Spectroscopy Data

The data here will assist in determining the type of recombination processes related to the light output of the samples. The experiments carried out on the emission spectroscopy of the samples may be divided into two parts:

(1) A simultaneous thermoluminescence run and wavelength scan of the peaks

(2) A simultaneous thermoluminescence run and intensity variation of the 590 nm or 750 nm peaks obtained in (1)

For experiments dealing with the simultaneous thermoluminescence run and wavelength scan of the peaks, the sample was gamma-irradiated for 13 hours at room temperature while it was in the sample holder. Then the sample holder with sample was inserted in the heating block and heating commenced. One recorder plotted the total thermoluminescence against the temperature. As the first TSL peak above room temperature

(360 K peak) was approached, the emission spectroscopy scanning was commenced. Wavelength scans of the lower temperature side, the peak, and the higher temperature side of the TSL peaks near 360, 430, and 450 K were made. Note these three TSL peaks are taken to correspond to the peaks 340, 430, and 450 K, respectively, of Sections A and B. Wavelength scans were also made between these TSL peaks. The highest attainable temperature with the heating apparatus was about 540 K. In general only two wavelength peaks centered at 590 nm and 750 nm were obtained. Some emission also occurred around 820 nm; this was prior to the onset of the 340 K peak. Figure 16 shows the wavelength scans typical of the undoped samples. Similar scans were obtained for the first three peaks above room temperature for the doped samples. These are shown in Figure 17. The first three TSL peaks occurring here above room temperature are again 340, 440, and 460 K. No emission bands other than the 590 nm and 750 nm bands were evident.

For the second class of emission spectroscopy experiments--a simultaneous thermoluminescence run and intensity variation of the 590 nm or 750 nm peaks obtained in the previous experiments--samples were gamma-irradiated for 13 hours as in the previous experiments, replaced in the heating block and heating commenced. Here again one recorder plotted the total TSL as in the previous experiments, but now the monochromator was set at 590 nm and a second recorder plotted the variation in the intensity of this band with time. Both the total TSL and the 590 nm emission are shown in Figure 18a for the undoped samples. Note that the relative TSL and 590 or 750 nm is plotted; no corrections have been made for the difference in photomultiplier tube or changes in spectral sensitivity of tube with wavelength. After the Gamma Run

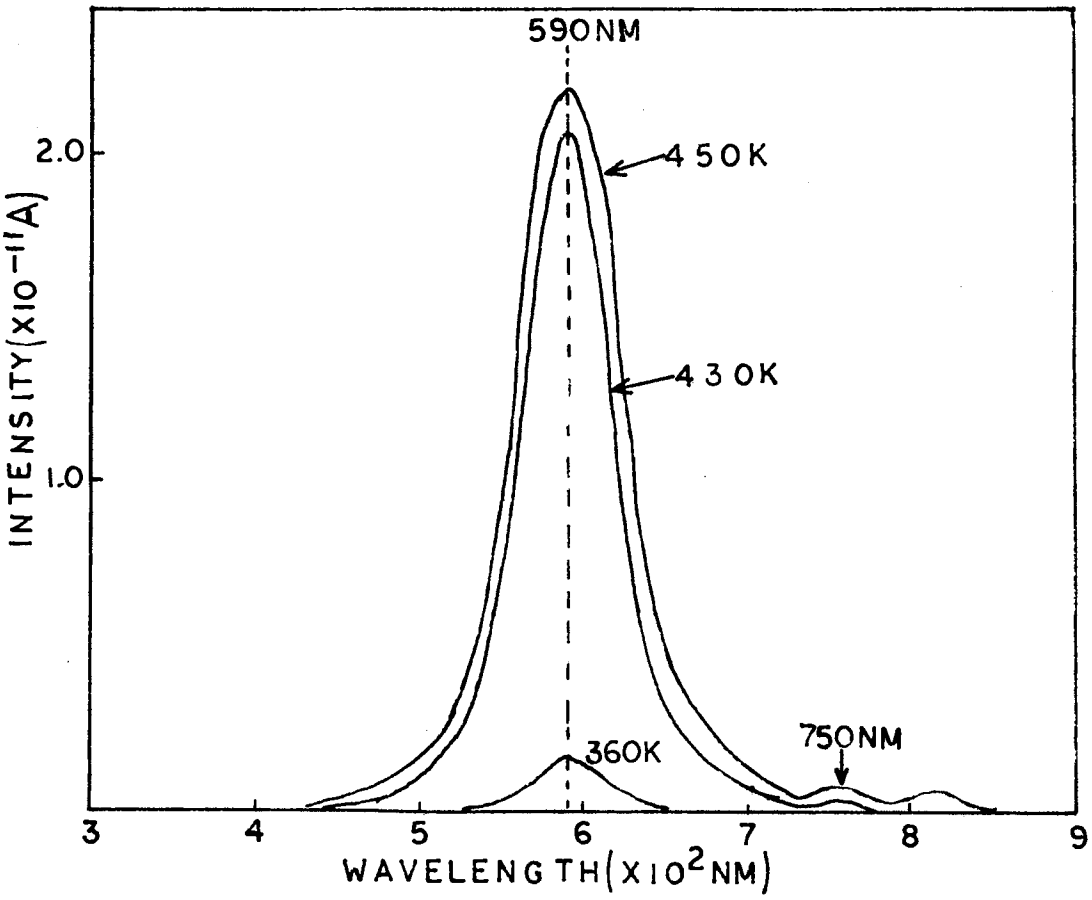

Figure 16. Spectral Distribution of the TSL Peaks: (a) 360 K, (b) 430 K, (c) 450 K Peaks of the Undoped Crystal, Irradiated at Room Temperature

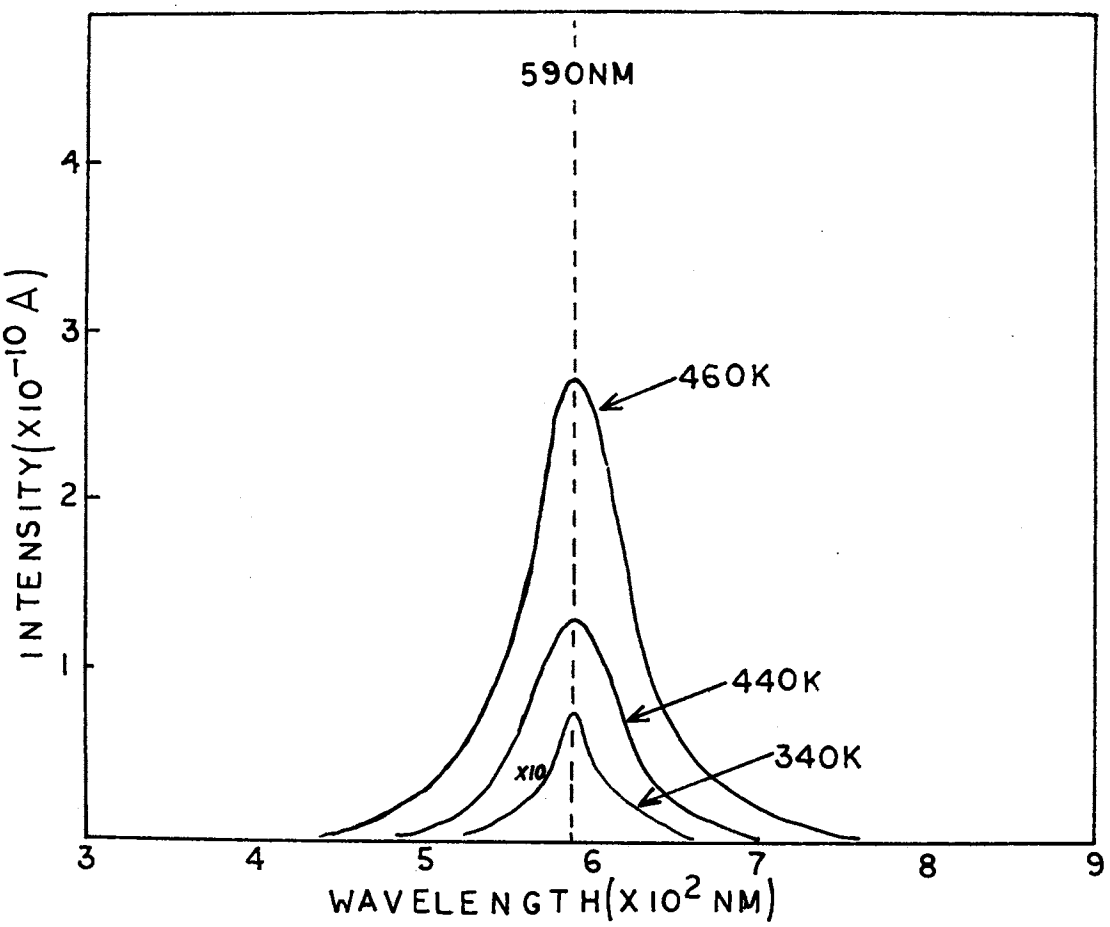

Figure 17. Spectral Distribution of the TSL Peaks: (a) 340 K, (b) 440 K, (c) 460 K Peaks for the Doped Crystal, Irradiated at Room Temperature

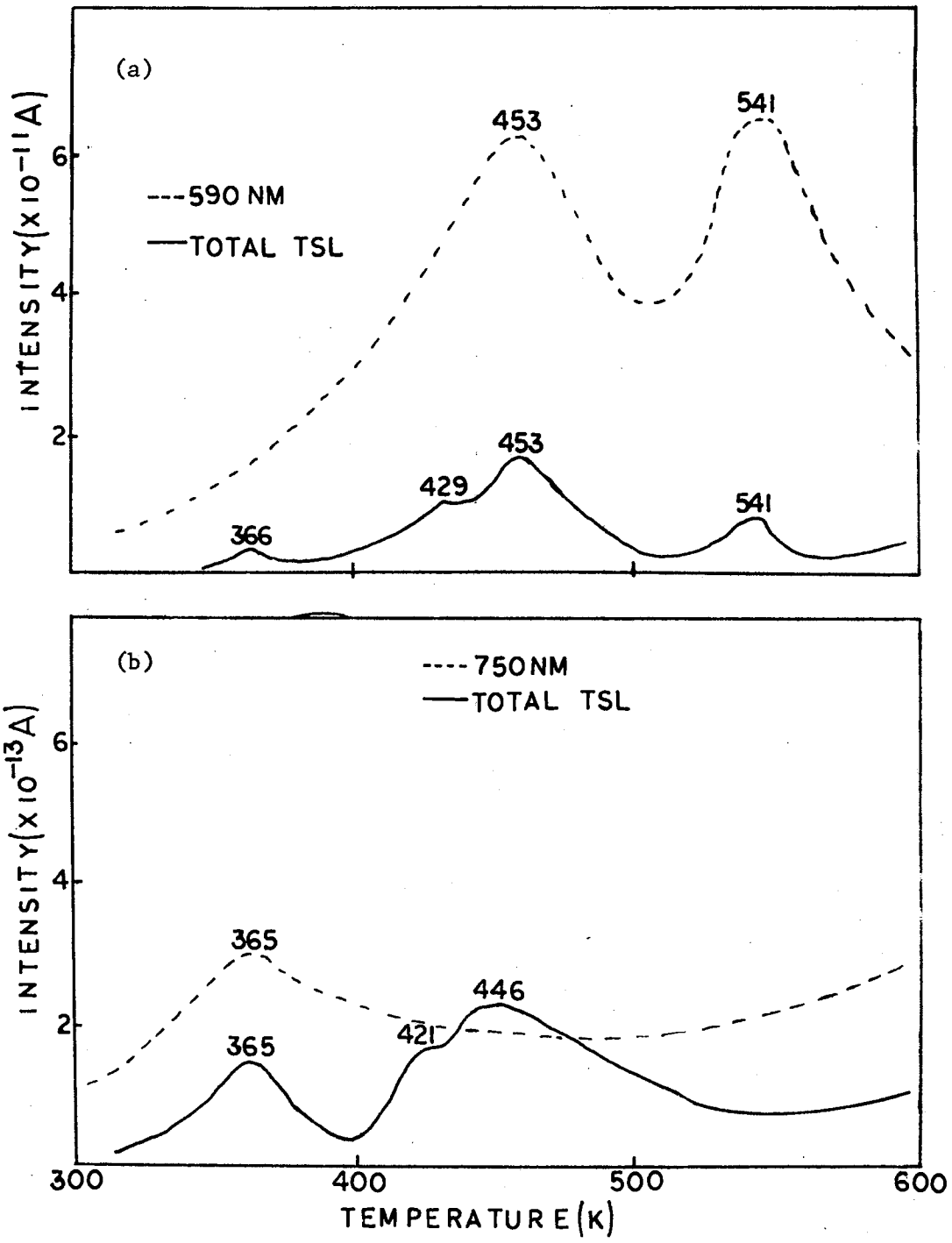

Figure 18. (a) Variation of the 590 nm and Total TSL With Temperature for the Undoped Crystal, Gamma-Irradiated at Room Temperature

(b) Variation of the 750 nm and Total TSL With Temperature for the Undoped Crystal, Excited by UV After Run (a)

above, the holder with the sample in position was taken out of the heating block, irradiated with UV light for one hour, and replaced. Then the monochromator was set at 750 nm and the total TSL and variation with time of the 750 nm emission were both monitored simultaneously. This result in shown in Figure 18b.

Again, the sample was gamma-irradiated for 13 hours, the total TSL and the variation with the 750 nm emission monitored simultaneously (Figure 19a). Finally, the sample and holder were removed from the heating block, irradiated with UV light for one hour, and replaced. The total TSL and time variation of the 590 nm intensity were monitored (Figure 19b).

The four experiments described above on the undoped samples and shown in Figures 18 and 19 were also carried out on the doped samples. The corresponding results are shown in Figures 20 and 21.

The results of the spectral composition of the TSL peaks may be summarized as follows. Where a double temperature is given for a peak, the first and second temperatures refer to the temperatures of occurrence in the undoped and manganese-doped samples, respectively.

1. In both samples the main spectral emission for the 360/340 K, 430/440 K, and 450/460 K peaks examined is in the 590 nm or 750 nm bands.
2. Except for the 360 K peak, there is a peak in the 590 nm emission spectrum corresponding to each TSL peak, and this emission is proportionately greater in the undoped sample.
3. There is a 750 nm emission only in the first two TSL peaks (360/340 and 430/440 K) above room temperature and this appears to be larger in the undoped sample.

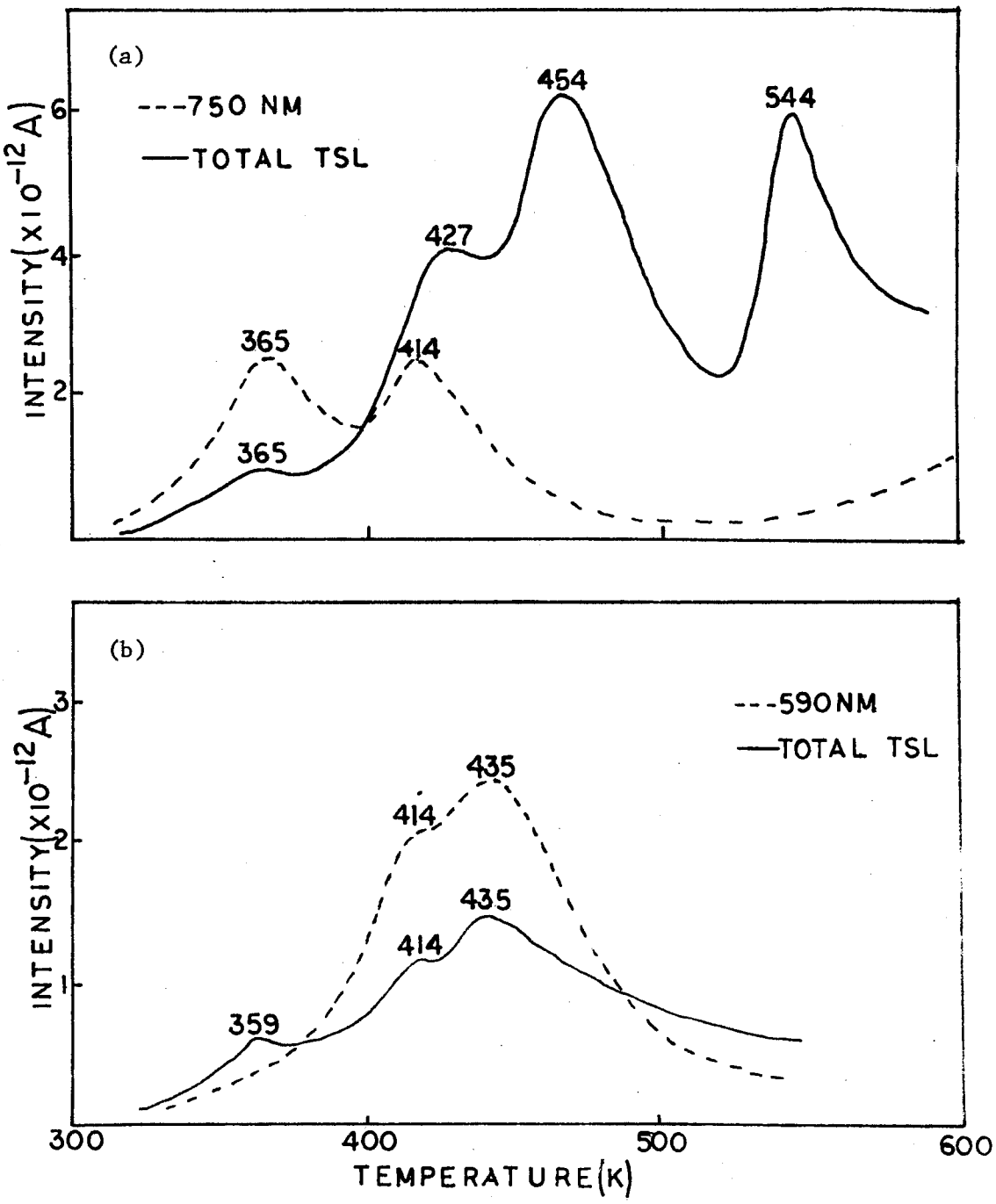

Figure 19. (a) Variation of the 750 nm and Total TSL With Temperature for the Undoped Crystal, Gamma-Irradiated at Room Temperature

(b) Variation of the 590 nm and Total TSL With Temperature for the Undoped Crystal Excited by UV After Run (a)

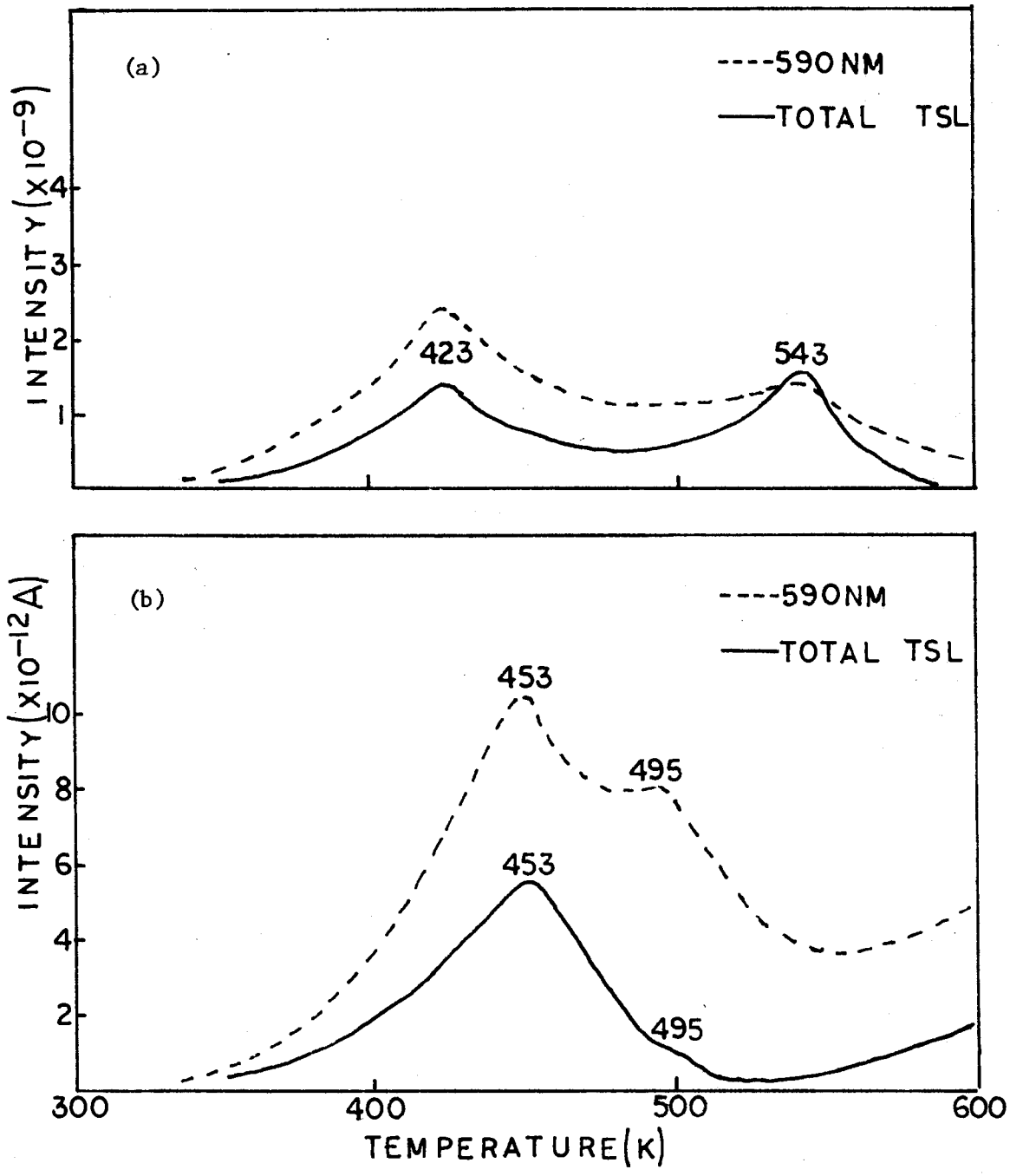

Figure 20. Variation of the 590 nm and Total TSL for the Doped Crystal (a) Gamma-Irradiated at Room Temperature and (b) Excited by UV After Run (a)

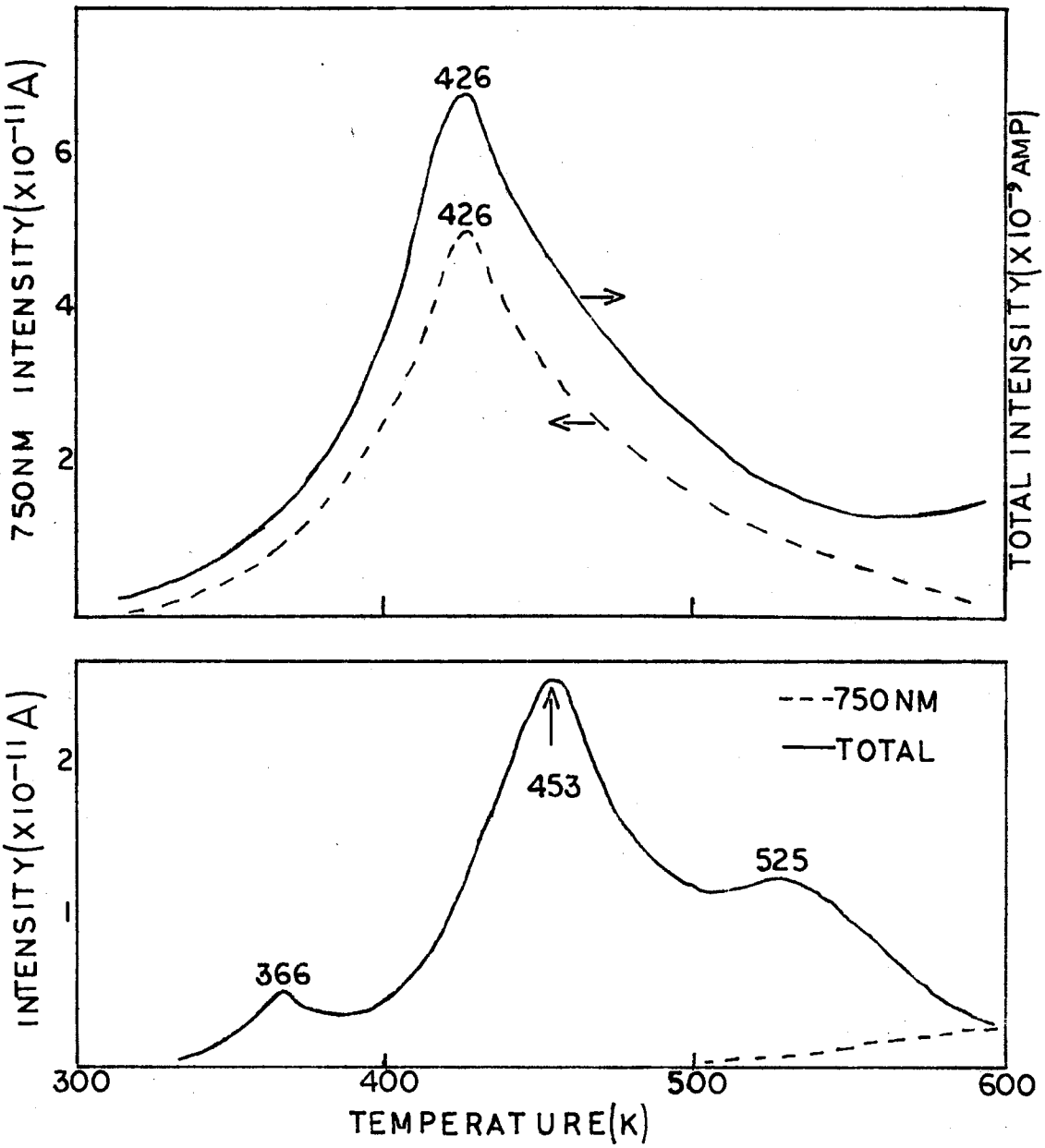

Figure 21. Variation of the 750 nm and Total TSL for the Doped Crystal: (a) Gamma-Irradiated at Room Temperature; (b) Excited by UV After Run (a)

Thus for all the samples the main luminescence centers are the 590 nm (Mn^{2+}) and the unknown 750 nm emission.

D. Illumination Into the F Band and Correlation With Optical Absorption

Undoped samples, on the slide used in Section C, were illuminated with the Cenco UV light using a 254 band pass filter. This approximates the F band (275 nm) in $KMgF_3$. In this and in all the illuminations described below, the distance from the exit slit of source to sample was kept constant at 6½ inches.

For the data in this section the sequence of events was as follows: First the sample was gamma-irradiated for eight hours, an optical absorption run made, the TSL Run followed, and a final optical absorption (O.A.) run made. The results of the O.D. runs before and after the TSL Run are shown by the points A (O.D. = 1.59) and B (O.D. = 0.76), respectively, in Figure 22. Note that the O.A. is plotted on the ordinate on the right-hand side. The TSL peak heights (left ordinate) of the first four peaks above room temperature are shown by the symbols ○, □, △, ● in Figure 22 on the vertical line corresponding to the treatments undertaken. This gamma-run just described forms the baseline for the treatments which follow.

Samples were annealed in the usual way before being gamma-irradiated for eight hours. Then an O.A. run was made, and the 254 nm light shone on the sample for 40 minutes as described above. This treatment is designated (gamma + 40). A TSL Run was made, and finally an O.A. run again made. The points C and D of Figure 22 represent the

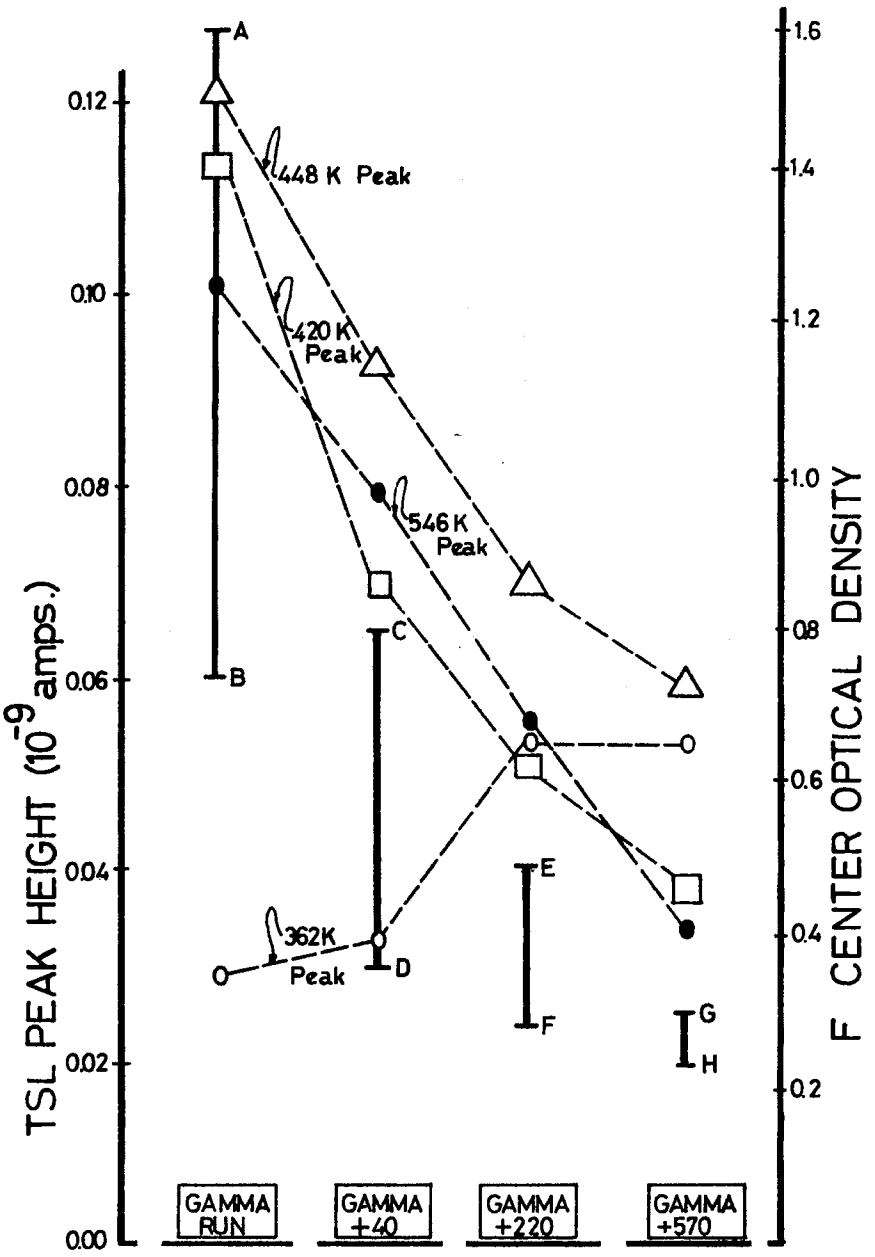

Figure 22. Variation of TSL Peak Height and F Center Optical Density With F Band Illumination

NOTE: In each case, the four points plotted on the vertical line represent (on the left ordinate) the TSL peak heights subsequent to the treatment specified. Thus the "Gamma Run" is a baseline. The points A and B, C and D, etc. represent (on the right ordinate) the optical densities before and after each TSL run. Specifically the point C is the F center O.D. after an F band illumination of 40 minutes, subsequent to the same initial gamma dose.

initial O.A., after UV illumination, and final O.A. after the TSL run, respectively.

Similarly point E represents the O.A. after eight hours gamma-irradiation and a subsequent 220 minutes 254 nm illumination. Point F is the final O.A. after the TSL run. In the third and final treatment (gamma + 570), represented by GH, the length of 254 nm illumination was 570 minutes. The baseline and the three treatments just described are designated gamma-run, gamma + 40, gamma + 220, and gamma + 570, respectively. No similar treatments were undertaken on the doped samples.

It is observed that when undoped samples are excited with 254 nm radiation (approximating the F band of 275 nm) following an initial gamma dose, the F center optical density is markedly decreased; in addition, the TSL peak heights, obtained subsequently, except the 362 K peak, are all smaller. These two trends are repeated when the length of F band illumination is increased from 40 to 570 minutes following the usual gamma dose.

E. Correlation of Thermal Annealing of F Centers and Optical Absorption

The series of experiments described below were designed to see how the concentration of F centers decreased as the temperature is increased. Thus annealing stages of the F center optical density may correlate with TSL peak temperatures.

One way to do this is to place the sample in a specially designed cell with heater in the compartment of the Cary 14 spectrophotometer and heat the sample while observing the F center absorption band. An

unknown effect here, however, is the broadening of the band with increase in temperature.

To circumvent this difficulty, the following procedure was followed: The sample was gamma-irradiated for three hours, run on the Cary 14, placed in the TSL system, and heated to the desired annealing temperature. Then the sample was cooled, and a Cary 14 run again made. This entire process was repeated for a series of annealing temperatures from about 370 to 670 K. Each of these experiments gave a value for the O.A. of the F center band at different temperatures. These are plotted in Figure 23 against the temperature. The point A on the extreme left of the figure is the $(O.D.)_F$ after an eight hour gamma-irradiation and no subsequent bleaching. The point B is the $(O.D.)_F$ after an eight hour gamma-irradiation and subsequent heating to 377 K and so on.

As the temperature increases the F center optical density decreases slightly from room temperature to about 380 K. There is a marked decrease in O.D. in the temperature range 110-180 K and a significant decrease in the region around 570 K. Throughout the temperature region 273-550 K the F_2 center optical density at first increases slightly up to around 450 K and afterwards decreases.

F. EPR Experiments

(1) Undoped samples were gamma-irradiated at room temperature, and the Mn^{2+} signal level noted at 77 K both before and after irradiation. The sample was then heated to 560 K and the Mn^{2+} signal level again monitored.

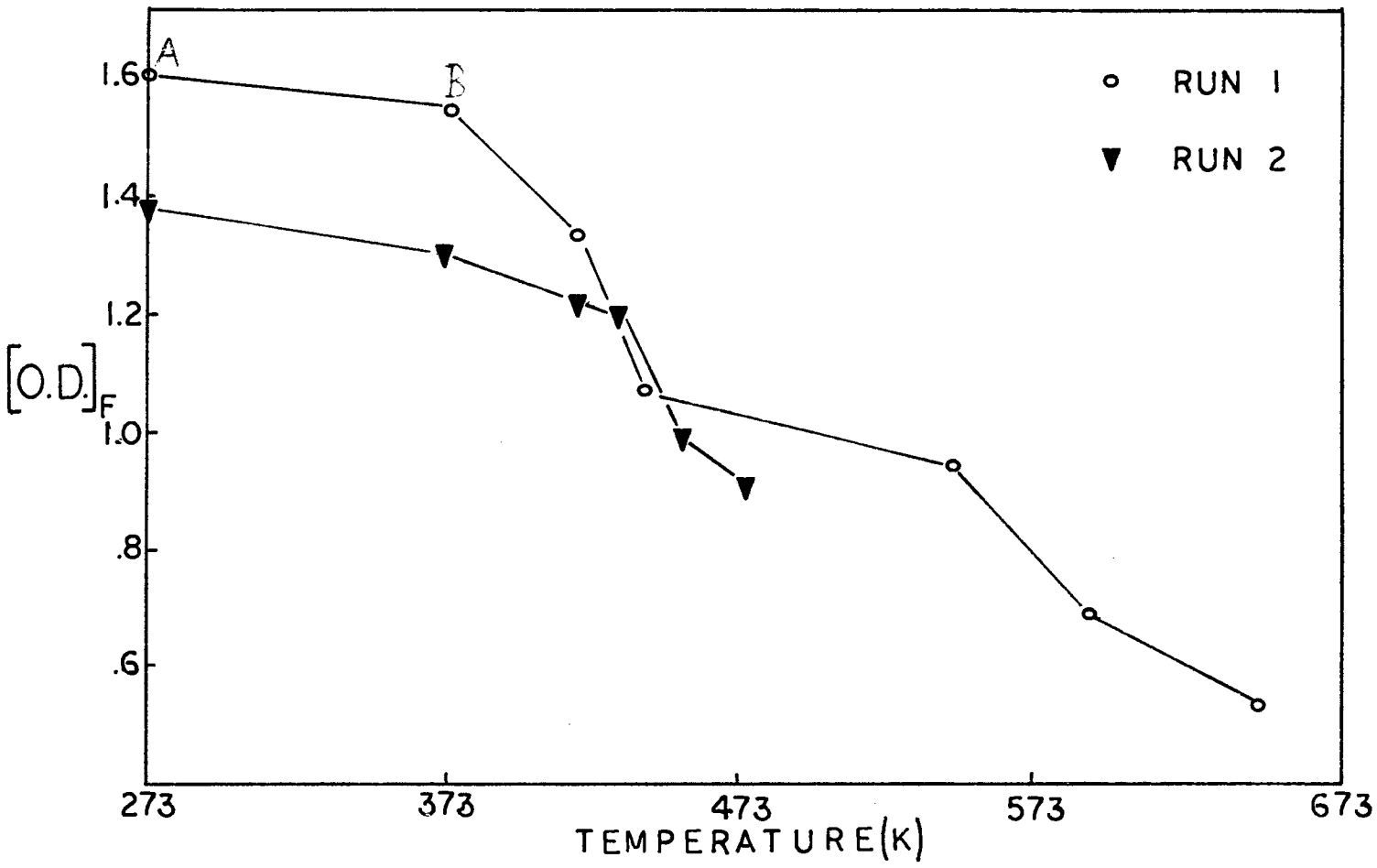

Figure 23. Variation of F Center Optical Density With Temperature Due to Thermal Annealing

In gamma or electron irradiated samples, comparison of signal levels indicated no significant change in the Mn^{2+} concentration occurred.

(2) Undoped samples were gamma-irradiated at room temperature, and ESR signals similar to V_K signals were observed. When samples were then excited at 77 K with unfiltered UV light, no signals similar to V_K signals were observed, but signals indicating the presence of other paramagnetic centers were seen. The origin of the latter signals is unknown at this time but is considered an important area for future work.

The main results of the EPR data are that any valence changes in Mn^{2+} occurred in amounts too small for gross observation and no V_K signals were seen upon excitation with UV at 77 K. Thus, the low temperature TSL peaks are not related to hole centers of the V_K type.

CHAPTER V

CONCLUSION AND DISCUSSION

A. Summary of Results

A summary of the observations of the previous chapter leads to certain general conclusions:

1. No TSL is produced by UV excitation except when the sample is given a prior dose of gamma-rays. This implies that F centers are necessary, perhaps indirectly, in the TSL process.
2. Generally speaking, the same TSL peaks seem to occur in both Mn^{2+} doped and undoped $KMgF_3$ samples, implying that the peak temperature is independent of the manganese doping. Except for the 360/340 K TSL peak, the peak heights increase with the Mn^{2+} doping and with the F center concentration, suggesting that the TSL output is dependent on both these quantities.
3. The peak heights of the first four TSL peaks, except the 360 K peak, above room temperature obtained after gamma irradiation followed by increasing F band illumination are successively smaller than those obtained in a regular "Gamma Run." This implies that these, except for the 360 K peak, are associated in some way with F centers.
4. The emission spectroscopy data shows that the same 590 nm emission occurs in the first four TSL peaks above room temperature. It should be noted that the first peak has significant

750 nm emission associated with it.

5. One result of the EPR work indicates that the low temperature TSL peaks are not related to any of the known types of V_K centers. Another result is any valence changes in Mn^{2+} occurred in amounts too small for gross observation.

B. Proposed Model

The results summarized above on the TSL of gamma and UV irradiated $KMgF_3$ are, of course, capable of many explanations. It is the purpose here to suggest certain simple elements of one tentative model which would seem to form a reasonable basis for further investigation of TSL and TSCE phenomena in comparable systems.

This model combines the ideas of Ausin and Alvarez Rivas (47) and Merz and Pershan (3) who investigated TSL in alkali halides above and below room temperature, respectively. The model is thus conveniently divided into two parts corresponding to these two temperature regions.

1. TSL Above Room Temperature

When $KMgF_3$ is gamma-irradiated at room temperature, F centers and their aggregates, as well as single and aggregated interstitials, are the main defect products (57). Unstable V_K centers may also be formed. Apparently no lattice defects are formed by UV irradiation of the sample at room temperature, although ionization of existing defects can occur.

When the sample is heated, the interstitials become increasingly mobile and move towards F centers. The interstitial fluorine atoms can recombine with the F centers leaving fluoride ions and an undetermined

amount of recombination energy. The released energy is transferred in such a way as to excite a nearby Mn^{2+} ion which on decay emits a 590 nm photon. A survey of manganese-doped alkali halides indicates that Mn^{2+} is the dominant luminescent center, and in $KMgF_3$ this ion emits in the 590 nm region (46). The following general reaction scheme gives the suggested chain of events.

$$F^{o} + \text{F center} + Mn^{2+} \longrightarrow (F^{-})^{*} + Mn^{2+}$$

(interstitial atom) (trapped electron in vacancy) (excited fluoride lattice ion)

$$\longrightarrow F^{-} + (Mn^{2+})^{*}$$

(normal lattice fluoride ion)

$$\longrightarrow F^{-} + Mn^{2+} + h\nu$$

(590 nm)

The first stage is assumed to be the formation of an excited fluoride ion in a regular lattice position; the excitation then goes to the Mn^{2+} and finally appears as a 590 nm photon. In this picture, the F centers play the role of fixed recombination centers, the interstitials being mobile entities which move towards the recombination centers.

In an alternative process, the lattice recombination energy may be transferred to a non-radiative recombination center resulting in the ejection of an electron (TSCE) from the crystal by an Auger mechanism. The proposed model requires the manganese and is consistent with (1) the larger TSL and smaller TSCE observed in the heavily manganese-doped samples and (2) the smaller TSL and larger TSCE in the undoped samples.

The origin of the 750 nm emission is not known at this time. It may well be the result of the transfer of the above-described lattice recombination energy to an F-aggregate or non-manganese impurity center. When undoped and Mn^{2+} doped $KMgF_3$ samples were gamma-irradiated at 77 K and allowed to warm up, another red emission was observed visually before the yellow-orange emission (presumably 590 nm) was seen. It has been suggested that this red emission may be due to perturbed Mn^{2+} (58).

The general rise and fall of the glow curve between 290 and 520 K is assumed to be explained by the interstitial-F center recombination and subsequent Mn^{2+} excitation. It remains to explain the origin of the small peaks superimposed on the glow curve and which are also obtained in successive UV re-excitations near 77 K. That they are not due to F center annealing is supported by the absence of annealing steps in the F center optical density curve. A possible mechanism could be the excitation by the UV at 77 K of an F center electron converting some of the Mn^{2+} to Mn^{1+}, the recombination of a hole (as yet unidentified) with the Mn^{1+} and subsequent Mn^{2+} excitation giving the characteristic manganese luminescence.

2. TSL Below Room Temperature

Again, it is important to realize that no low temperature TSL is seen unless the specimen has been pre-irradiated with gamma rays (or MeV electrons) at room temperature. A plausible explanation for the observed phenomena is that subsequent UV irradiation at 77 K causes electrons to be excited out of F centers. These electrons may combine with Mn^{2+} ions, converting them to Mn^{1+}, and they may also be trapped by other impurities. As the sample warms up, holes other than V_K type

centers may be thermally excited from traps recombining with Mn^{1+}, thus regenerating Mn^{2+} and providing the characteristic luminescence. The amount of Mn^{1+} may well be in too small concentration to be readily detected by EPR.

A corresponding mechanism here for the TSCE would be the recombination of a bound hole with a non-radiative recombination center other than a Mn^{1+} ion with ultimate transfer of energy to an electron in a neighboring center and subsequent ejection of this electron from the crystal.

Unfortunately, a great deal more work must be done before appropriate hole centers and Auger recombination centers can be identified to confirm this hypothesis. It is considered significant, however, that TSCE can be obtained with UV irradiation alone while TSL apparently depends upon the presence of F centers.

C. Discussion

Some additional arguments exist to support the model outlined above.

One important feature is the apparent similarity in TSL peak temperature of both the undoped and Mn^{2+} doped $KMgF_3$ samples. This was apparent also in lightly irradiated Mn^{2+} doped samples and undoped samples which were heavily irradiated. Another supporting feature is that the 590 nm emission follows very closely the total TSL. A third aspect is that in the "Gamma Runs" and "UV Runs" the former had barely separated peaks with a high interpeak background whereas the latter generally had a more separated appearance. This would be expected from the gradually increasing mobility of interstitials in contrast to the

sharper peak structure expected of electrons and holes released from traps.

Again, if electrons were released from F centers, this would imply as many different F centers as TSL peaks. Furthermore, F center electrons are tightly bound and are not expected to become freed by increasing temperature alone.

In this work is was found that no V_K centers were observed after UV irradiation subsequent to 295 K gamma irradiation. Both Riley (44), using electron irradiation at 7 K, and Altshuler and co-workers (45), using X-irradiation at 77 K, obtained low temperature TSL peaks, all of which agree well in temperature except for Riley's peaks below 77 K. It now seems reasonable to say, because of recent work on intrinsic and perturbed V_K centers in $KZnF_3$ (59), that the TSL peaks in the region 77 - 300 K of these authors are related to these hole centers. Although the 160 K peak observed in the work agrees well in temperature to that of the above-mentioned authors, this is probably coincidental, and no significance should be attached thereto.

D. Suggestions for Further Study

The following experiments would be most helpful in order to either support or disprove the model outlines.

1. It would be desirable to determine more exactly the association between steps (if any) of the thermal annealing curve and changes in the F center concentration. This can be done by observing the F center optical density at a greater number of temperatures from room temperature to 600 K.

2. The TSL peak structure and emission spectroscopy of compounds such as $NaMgF_3$, $KZnF_3$, and $KMgF_3$ doped with other impurities should be investigated. This data will show the dependence of peak temperature and spectral emission on cation and dopant.
3. The variation of TSL peak height and F center optical density with gamma-ray dose for both samples deserves more careful measurement. In particular the relationship between the integrated TSL intensity (as measured by the area under the TSL intensity versus temperature curve) and F center optical density would assist in challenging the proposed model for the thermoluminescence above room temperature.
4. It is important to find out if the TSL peaks produced by gamma-rays or electron irradiation at 77 K are the same as those obtained by gamma irradiation at room temperature followed by UV at 77 K. Equipment has been designed for this study and will soon be operational.
5. Experiments on TSC could be carried out by adapting the gas flow counter apparatus. The existance of TSC would indicate a charge carrying mechanism in contrast to the recombination of interstitials with F centers as suggested in the model outlined.

SELECTED BIBLIOGRAPHY

1. Cameron, J. R., et al, Thermoluminescent Dosimetry, University of Wisconsin Press (1968).

2. Dutton, D., and R. Maurer, Phys. Rev., 90, 126 (1953).

3. Merz, J. L., and P. S. Pershan, Phys. Rev., 162, 217 (1967).

4. Wyckoff, R. W. G., Crystal Structures, 2nd ed., Vol. 2 (Interscience, New York, 1964), p. 392.

5. Yun, S. I., private communication.

6. Riley, C. R., and W. A. Sibley, Phys. Rev., B1, 2789 (1970).

7. Hall, T. P. P., Brit. J. Appl. Phys., 17, 1011 (1966).

8. Hall, T. P. P., and A. Leggeat, Solid State Comm., 7, 1657 (1969).

9. Di Bartolo, B., Optical Interactions in Solids, Ed. W. B. Fowler (Academic Press, New York, 1968).

10. Pooley, D., Solid State Comm., 3, 241 (1965); Proc. Phys. Soc. (London), 87, 245 (1966).

11. Hersh, H. N., Phys. Rev., 148, 928 (1966).

12. Mott, N. F., and R. W. Gurney, Electronic Processes in Ionic Crystals, Oxford University Press (1940).

13. Garlick, G. F. J., and A. F. Gibson, Proc. Roy. Soc., 60, 574 (1948).

14. Braunlich, P., J. Appl. Phys., 38 (6), 2516 (1967).

15. Nicholas, K. H., and J. Woods, Brit. J. Appl. Phys., 15, 783 (1964).

16. Randall, J. T., and M. H. F. Wilkins, Proc. Roy. Soc., A184, 366 (1945).

17. Grossveiner, L. J., J. Appl. Phys., 24, 1306 (1953).

18. Lushchik, Ch. B., Dokl. Akad. Nauk. SSSR, 101, 641 (1955).

19. Haering, R. R., and E. N. Adams, Phys. Rev., 117, 451 (1960).

20. Halperin, A., et al, Phys. Rev., 117, 416 (1960).

21. Braunlich, P., Ann. Phys. (Germ.), 12, 262 (1963).

22. Booth, A. H., Canad. J. Chem., 32, 214 (1954).

23. Bohun, A., Czech. J. Phys., 4, 91 (1954).

24. Hoogenstraaten, W., Phillips Res. Rep., 13, 515 (1958).

25. Braunlich, P., Proc. Conf. "Application of Thermoluminescence to Geological Problems," Spoleto, Italy (1966).

26. Saunders, I. J., J. Phys. C. (Solid State), 2 (2), 2181 (1969).

27. De Muer, D., Physica, 48, 1 (1970).

28. Kelly, Paul, et al, Phys. Rev. B., (3), 4 (6), 1960 (1971).

29. Kramer, J., Z. Phys., 133, 629 (1952).

30. Delchar, J. A., J. Appl. Phys., 38, 2403 (1967).

31. Fintelmann, K., Proc. 4th Czech. Conf. Electronic Vac. Phys., Prague (1968), p. 395.

32. Gessell, T. F., et al, Surf. Sci., 20, 174 (1970).

33. Holzapfel, G., Phys. Stat. Sol., 33, 325 (1969).

34. Bohun, A., Czech J. Phys., 4, 89 (1954).

35. Kreigseis, W., and A. Schamann, Phys. Stat. Sol., 33, K41 (1969).

36. Holzapfel, G., and J. Kramer, PTB-Mitt., 80 (5), 318-354 (1970).

37. Tolpygo, E. I., et al, Izv. Akad, Nauk. SSSR, Ser. Fiz, 30, 1980 (1966).

38. Mollenkopf, H. C., Ph.D. disseration, Oklahoma State University (1973).

39. Brotzen, F. R., Phys. Stat. Sol., 22, 9 (1967).

40. Bohun, A., PTB-Mitt., 80 (5), 320-329 (1970).

41. Becker, K., CRC Critical Reviews in Solid State Sciences, 3 (1), 39-81 (1972).

42. Balarin, M., and A. Zetzsche, Phys. Stat. Sol., 2, 1760 (1962).

43. Kelly, Paul, Phys. Rev. (3), 5 (2), 749 (1972).

44. Riley, C. R., Ph.D. dissertation, University of Tennessee (1970).

45. Altshuler, N. A., et al, Optika Spectroscopiya, 33 (2), 207 (1972).

46. Riley, C. R., et al, Phys. Rev. B., 5 (8), 3285 (1972).

47. Ausin, V., and J. L. Alvarez-Rivas, J. Phys. "C" (Solid State), 5, 82 (1972).

48. Damask, A. C., and G. J. Dienes, Point Defects in Metals (Gordon and Breach, New York, 1963).

49. Jain, S. C., and P. C. Mehendru, Phys. Rev., A140, 957 (1965).

50. Radhakrishna, S., and R. Narayanan, Phys. Stat. Sol. (a), 19, 103 (1973).

51. Sonder, E., et al, Phys. Rev., 159 (3), 755 (1967).

52. Goldberg, P., Luminescence of Inorganic Solids, Academic Press (1966).

53. Shvarts, K. K., and G. K. Vale, Izv. Akad. Nauk. SSSR, Ser. Fiz, 25, 333 (1961).

54. Osiko, V. V., Opt. i Spektr. Suppl., 1, 135 (1967).

55. Botden, T. P. J., Phillips Res. Rep., 7, 197 (1952).

56. Dexter, D. L., J. Chem. Phys., 21,836 (1953).

57. Sonder, E., and W. A. Sibley, Point Defects in Solids, Vol. 1, Ed. J. H. Crawford (JR) and L. M. Slifkin, Chap. 4 (New York: Plenum Press, 1972).

58. Sibley, W. A., private communication.

59. Kappers, L. A., and L. E. Halliburton, J. Phys. C. (Solid State), 7, 589 (1974).

VITA

James Anthony MacInerney

Candidate for the Degree of

Doctor of Philosophy

Thesis: A STUDY OF THERMALLY STIMULATED LUMINESCENCE AND THERMALLY STIMULATED CHARGE EMISSION IN $KMgF_3$

Major Field: Physics

Biographical:

Personal Data: Born in Dublin, Ireland, July 16, 1940, the son of Eric P. and Annie MacInerney.

Education: Graduated from Gormonston College, County Meath, Ireland, in June, 1958; received the Bachelor of Science (General) degree from University College, Dublin, Ireland, in 1962; received the Master of Science degree from Oklahoma State University, July, 1969, with a major in Physics; completed requirements for the Doctor of Philosophy degree in July, 1974.

Professional Experience: Assistant Chemist with Samuel Jones and Co., Ltd., London S.E. 15 England, 1962-1963; Physics Instructor at the College of Technology, Kevin Street, Dublin, 1963-1966 and 1969-1970; Graduate Teaching Assistant, 1966-1969 and 1970-1972 Oklahoma State University; Graduate Teaching Associate, 1972-1973 in the Department of Physics, Oklahoma State University; Teaching Master at Seneca College of Applied Arts and Technology, Willowdale, Ontario, 1973-1974.